Karlsruhe Institute of Technology

Actinide electronic structure and speciation using high energy resolution X-ray absorption and emission spectroscopy

Tonya Vitova

Karlsruhe Institute of Technology, Institute for Nuclear Waste Disposal

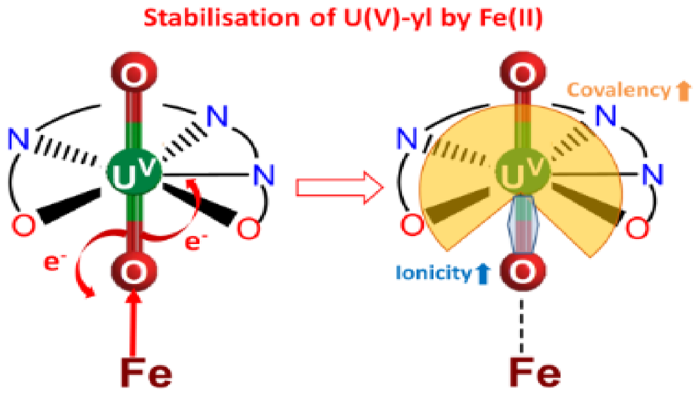

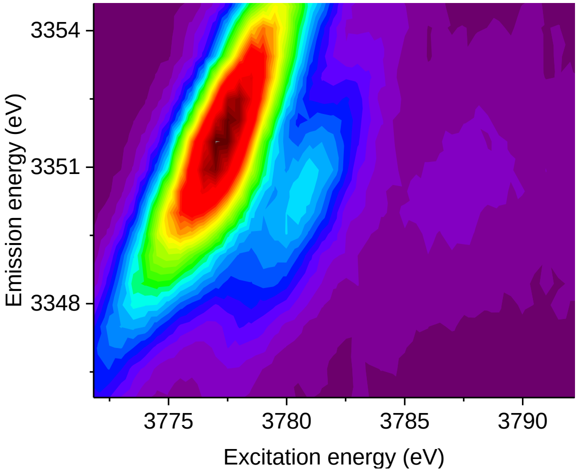

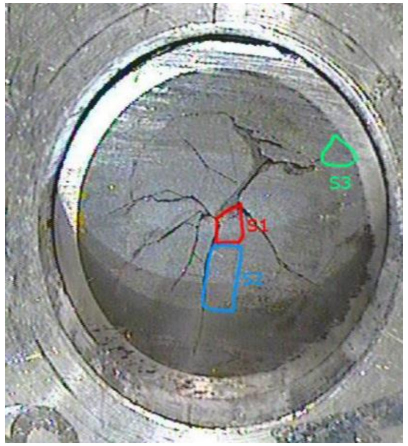

Basic principles of the High Resolution X-ray Absorption Near Edge Structure (HR-XANES) technique

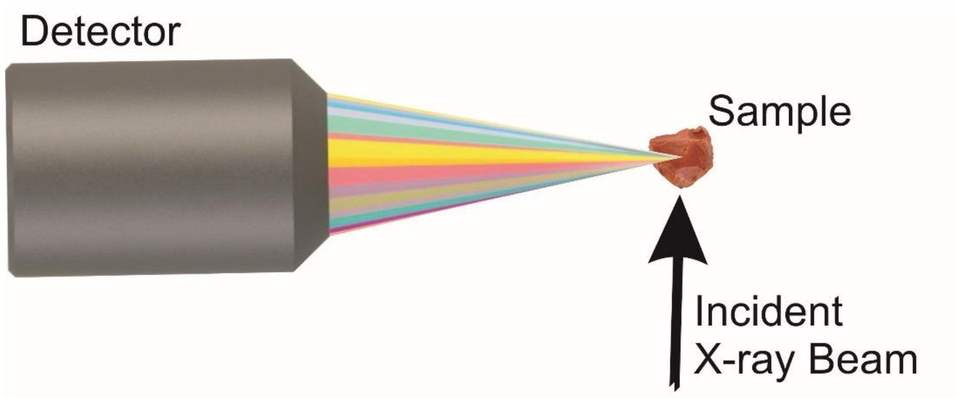

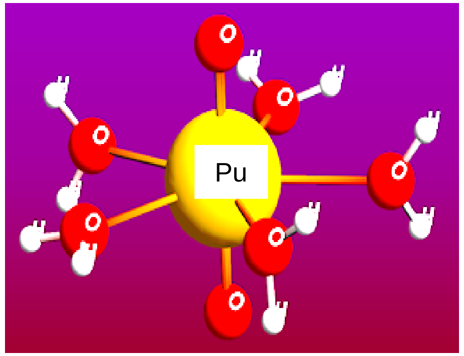

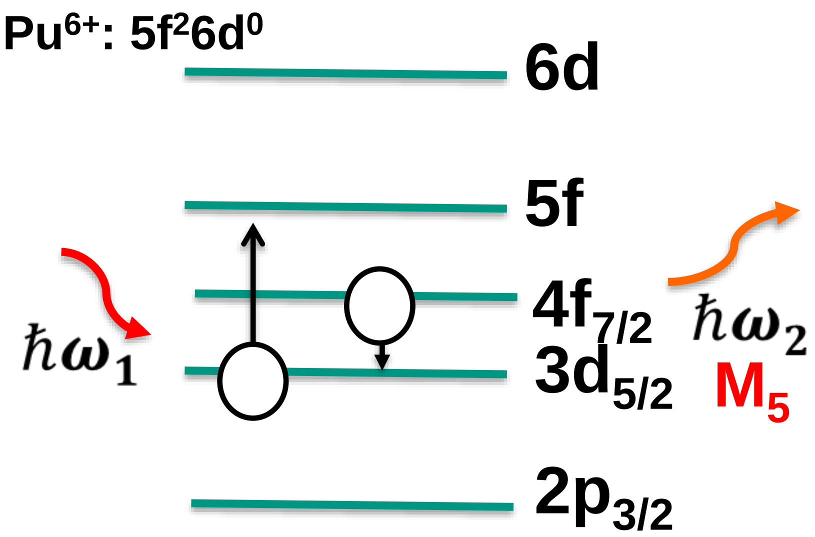

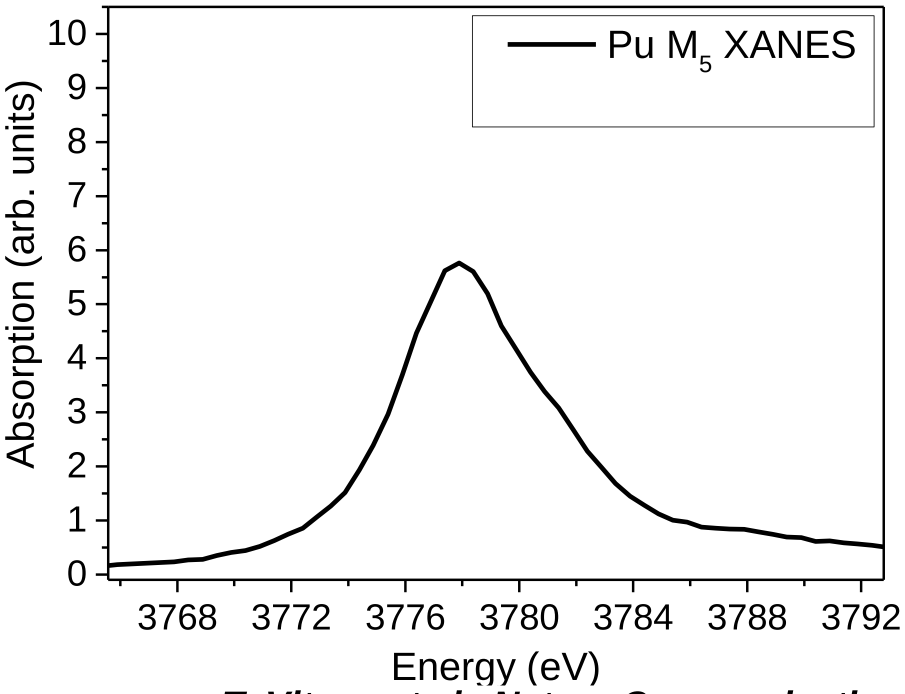

Dipole selection rule: $\Delta l = \pm 1$, $\Delta s = 0$, $\Delta J = \pm 1$

T. Vitova et al., Nature Communications 8 (2017) 16053

Basic principles of the High Resolution X-ray Absorption Near Edge Structure (HR-XANES) technique

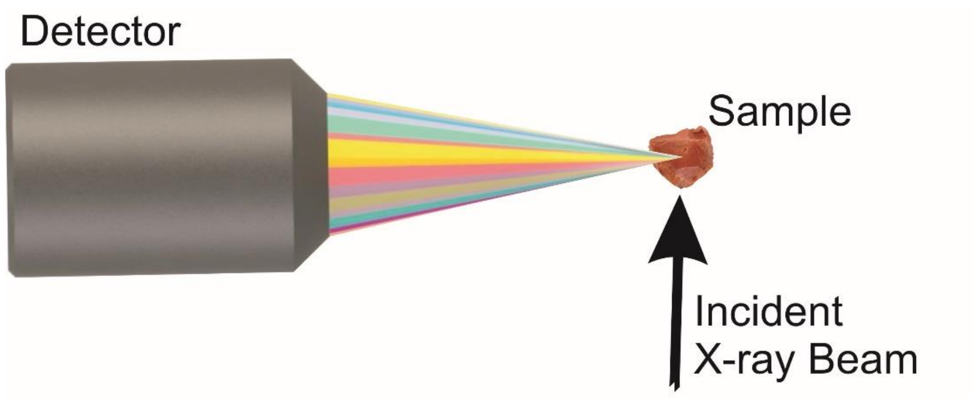

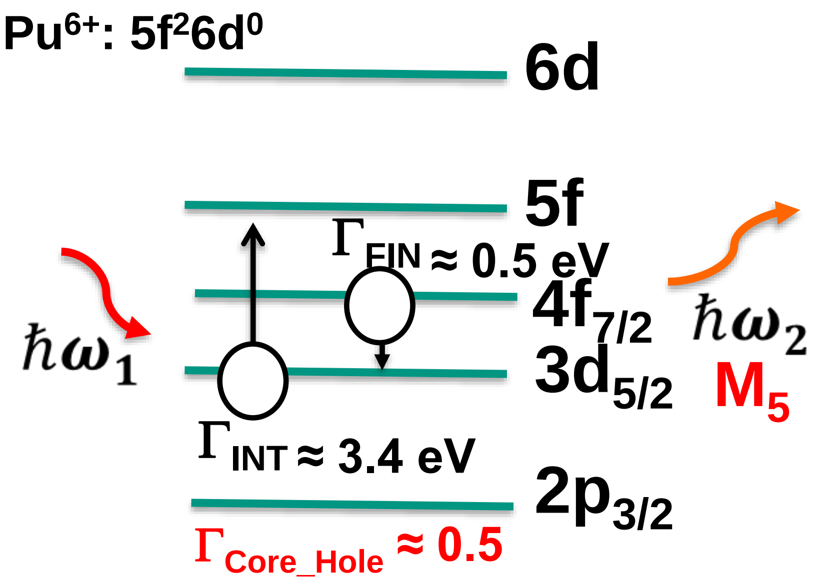

Dipole selection rule: $\Delta l = \pm 1$, $\Delta s = 0$, $\Delta J = \pm 1$

Energy resolution of Detector > 100 eV

spectral broadening (detector, beamline, core-hole lifetime broadening)

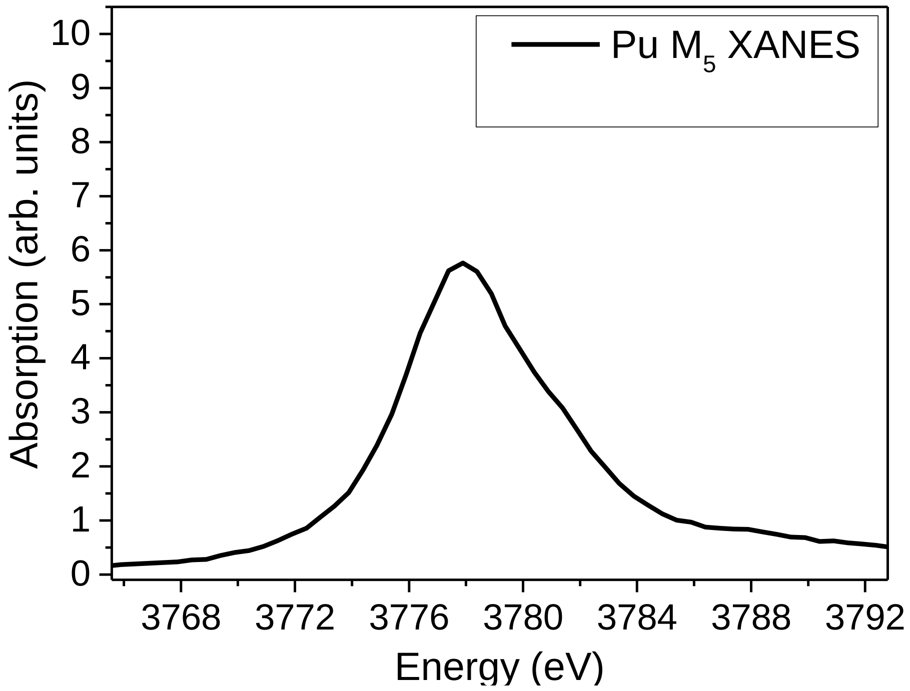

T. Vitova et al., Nature Communications 8 (2017) 16053

Basic principles of the High Resolution X-ray Absorption Near Edge Structure (HR-XANES) technique

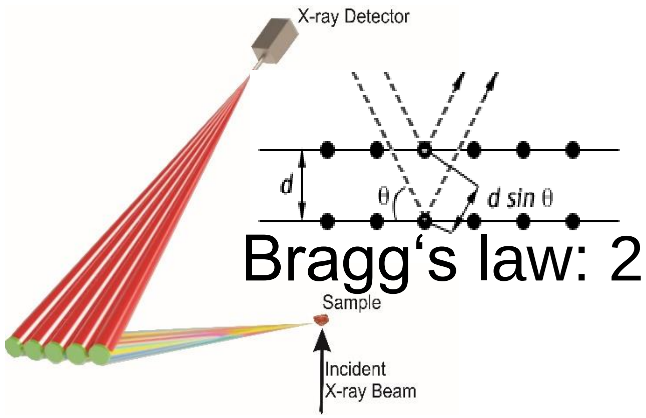

Bragg‘s law: $2d\sin\theta = n\lambda$

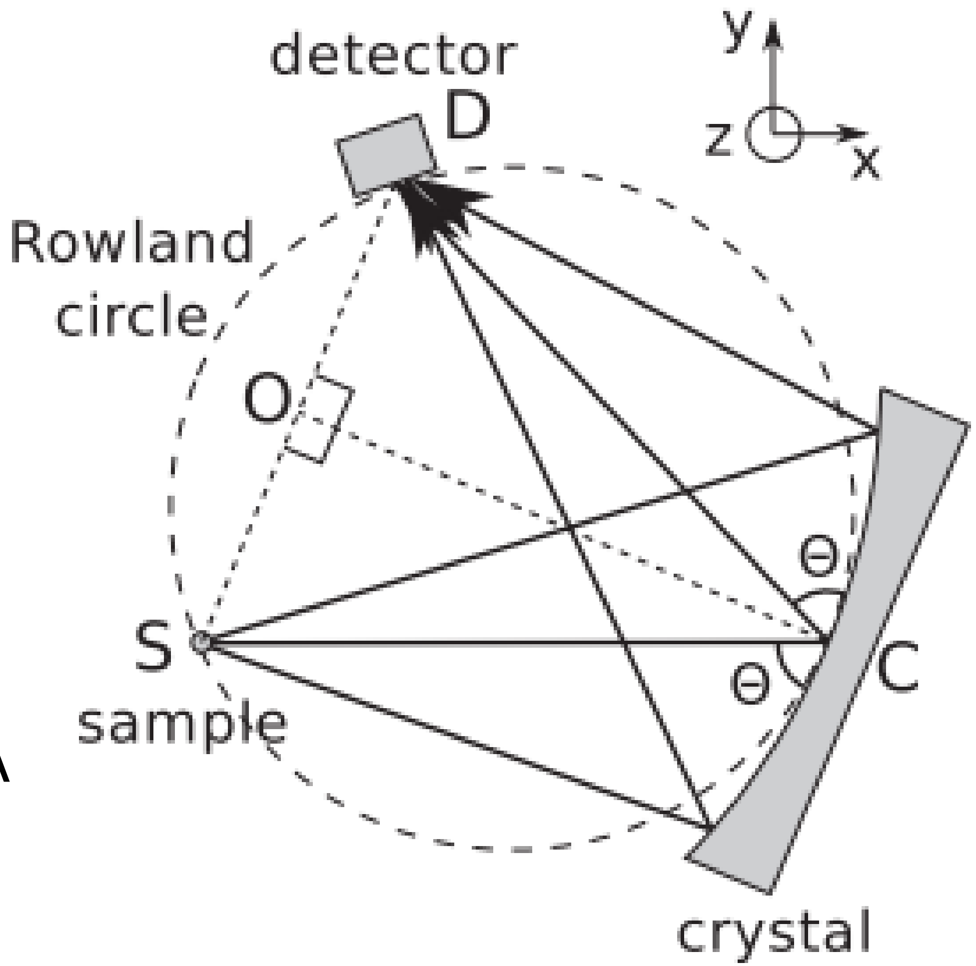

E. Kleymenov et al., Review of Scientific Instruments 82, 065107 (2011)

Basic principles of the High Resolution X-ray Absorption Near Edge Structure (HR-XANES) technique

Karlsruhe Institute of Technology

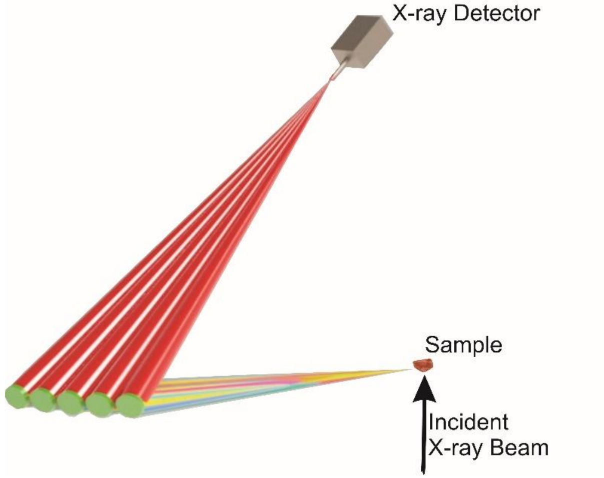

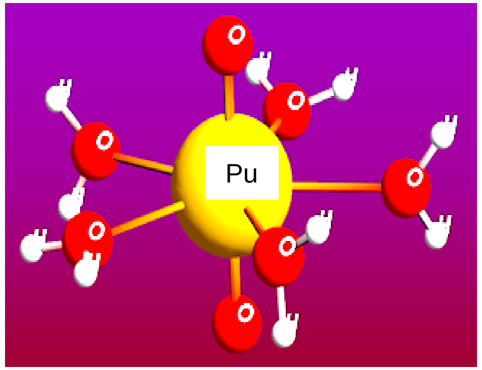

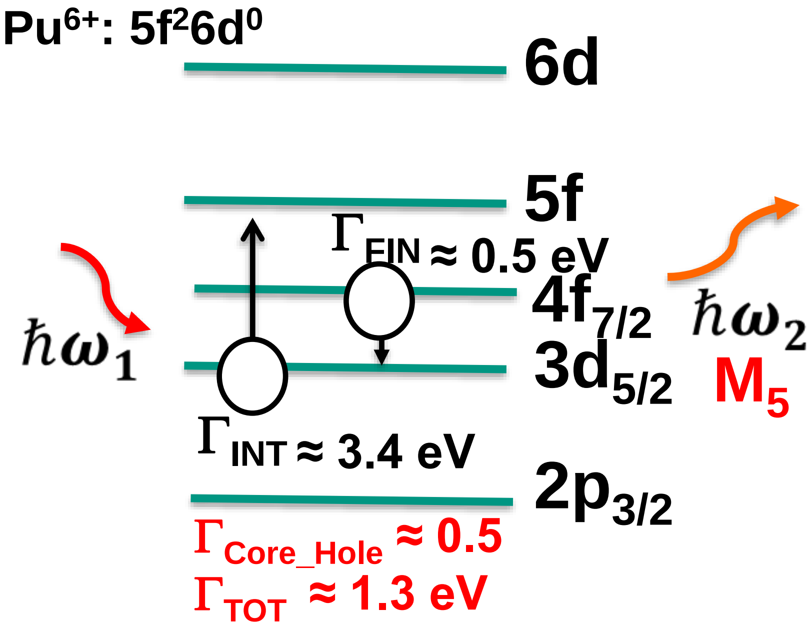

Energy resolution of Detector < 2 eV

spectral broadening (detector, beamline, core-hole lifetime broadening)

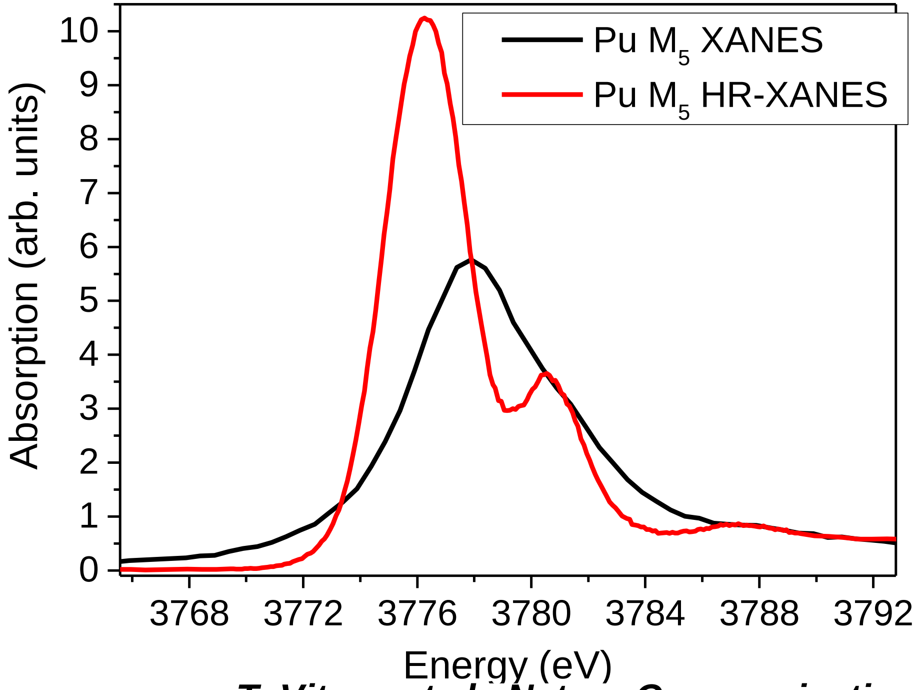

Dipole selection rule: $\Delta l = \pm 1$, $\Delta s = 0$, $\Delta J = \pm 1$

T. Vitova et al., Nature Communications 8 (2017) 16053

Basic principles of the Resonant Inelastic X-ray Scattering (RIXS) technique

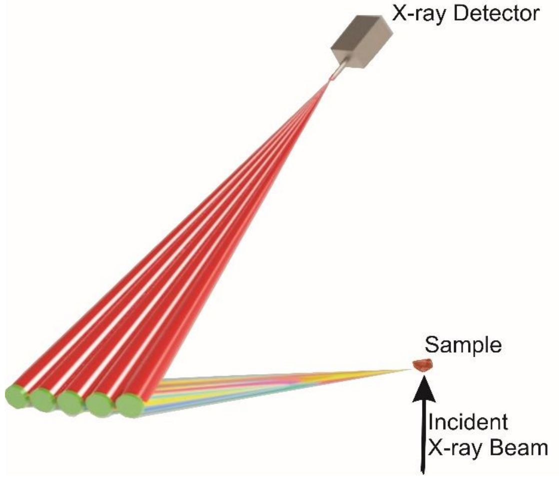

Pu^{6+}: $5f^2 6d^0$

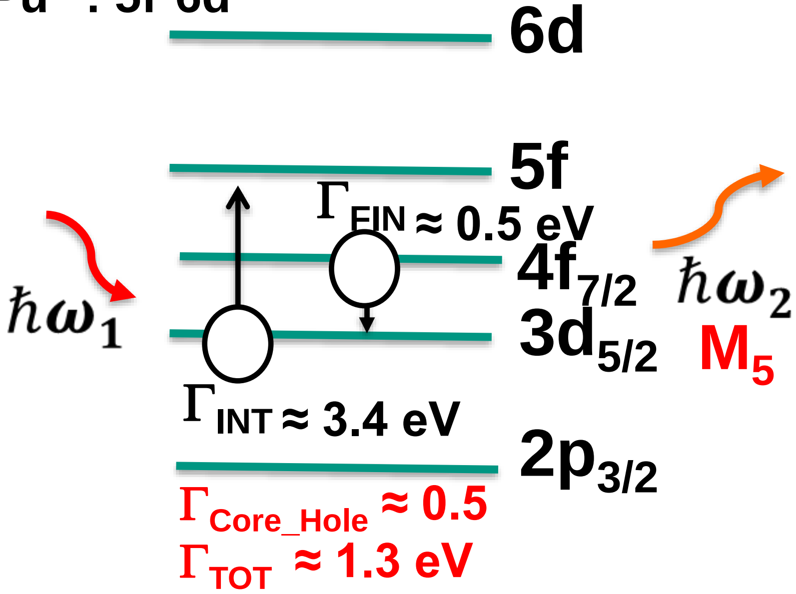

Dipole selection rule: $\Delta l = \pm 1$, $\Delta s = 0$, $\Delta J = \pm 1$

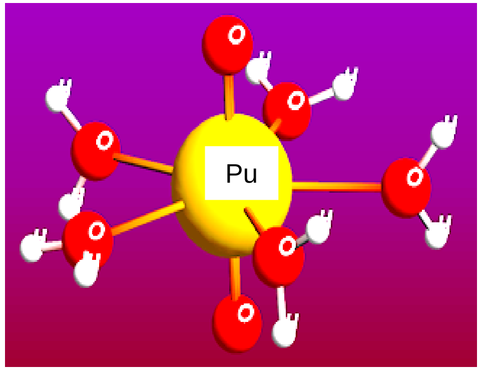

3d4fRIXS

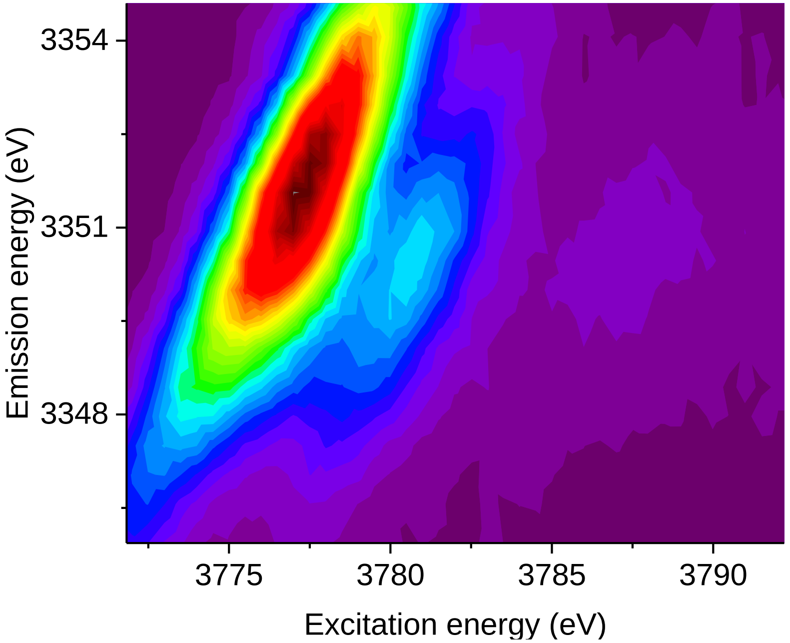

T. Vitova et al., Nature Communications 8 (2017) 16053

The high resolution X-ray emission spectrometer at the ACT stations at the KIT Light Source

INE and CAT-ACT-Beamlines: licenced for handling of radionuclides with activities up to 10^6 times the exemption limit

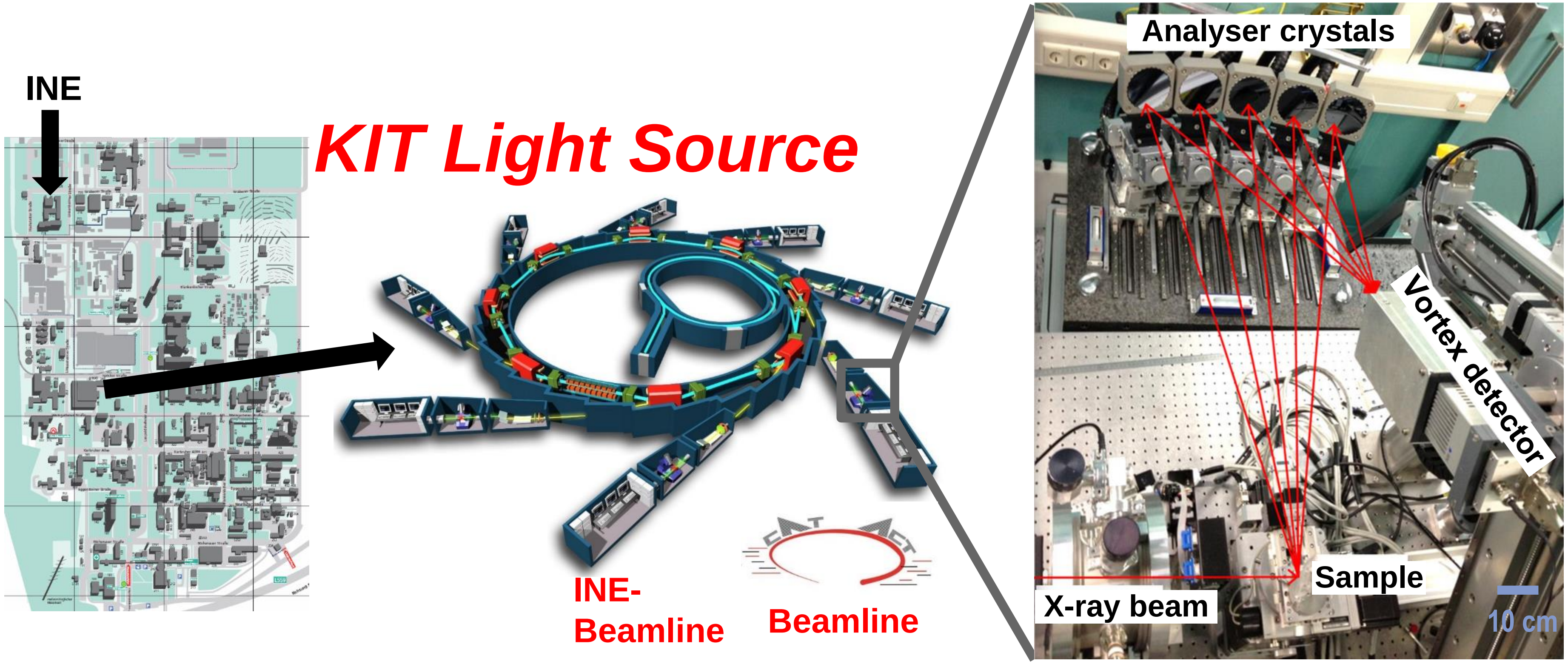

Zimina, A. et al. Review of Scientific Instruments 88, 113113 (2017)
Schacherl, B. et al. Anal. Chim. Acta 2022, 1202, 339636.
Schacherl, B. et al. J. Synchrotron Radiat. 2022, 29 (1), 80–88.

The high resolution X-ray emission spectrometer at the ACT stations at the KIT Light Source

Old spectrometer

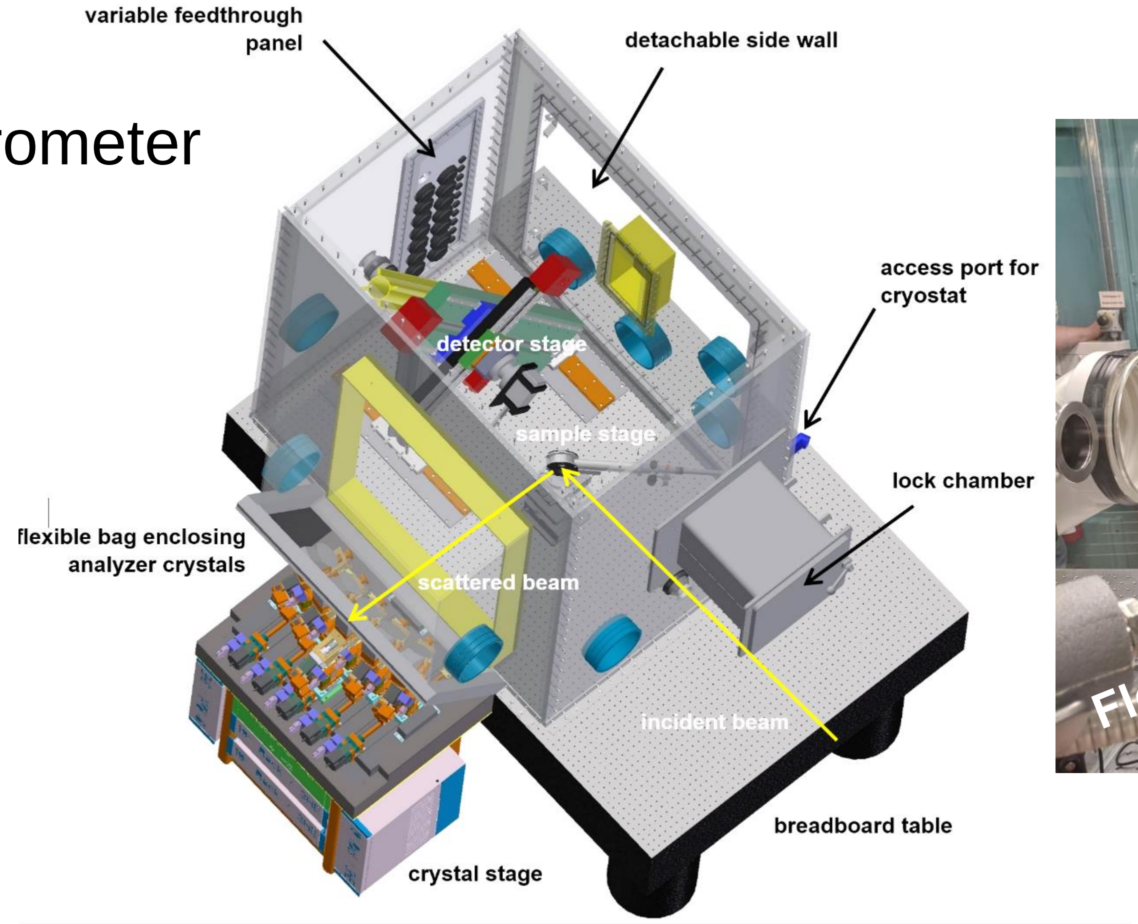

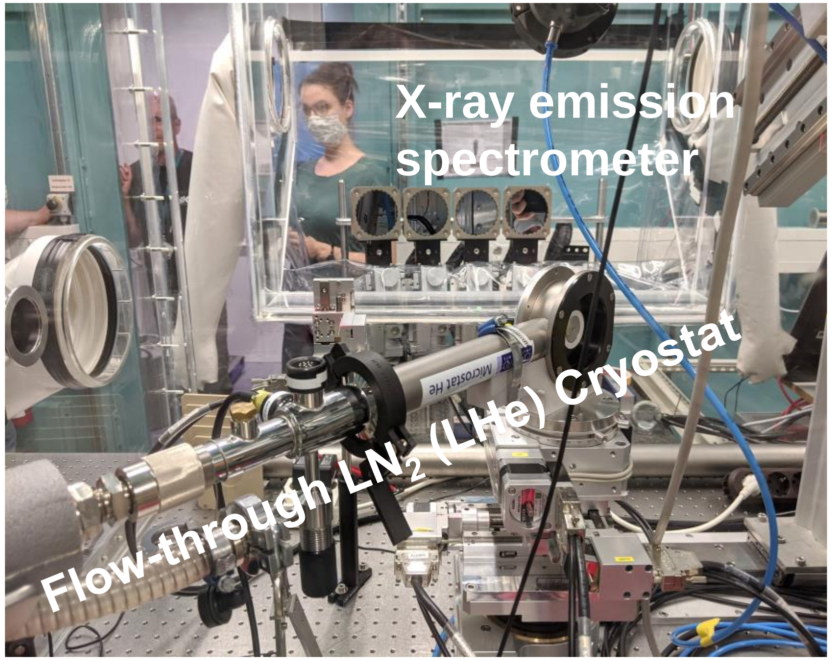

Zimina, A. et al. Review of Scientific Instruments 88, 113113 (2017)
Schacherl, B. et al. Anal. Chim. Acta 2022, 1202, 339636.
Schacherl, B. et al. J. Synchrotron Radiat. 2022, 29 (1), 80–88.

The high resolution X-ray emission spectrometer at the ACT stations at the KIT Light Source

NEXT spectrometer

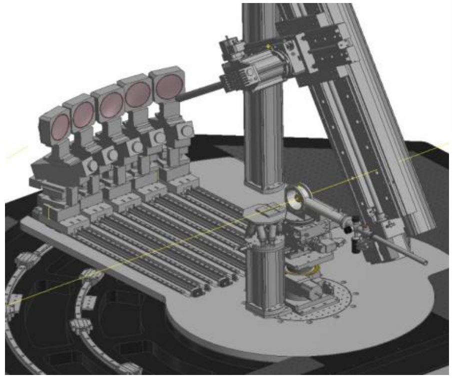

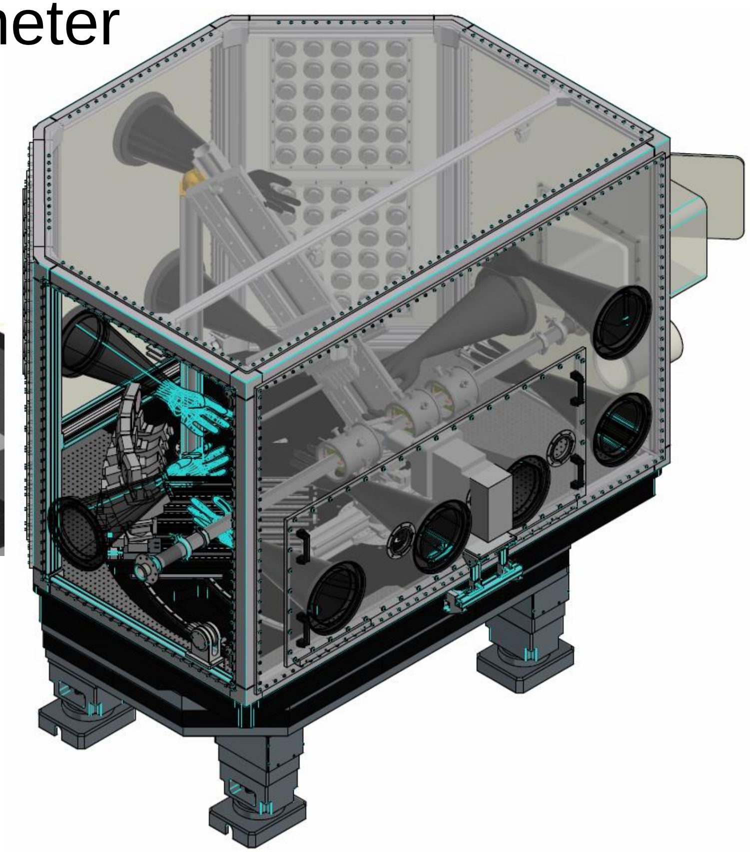

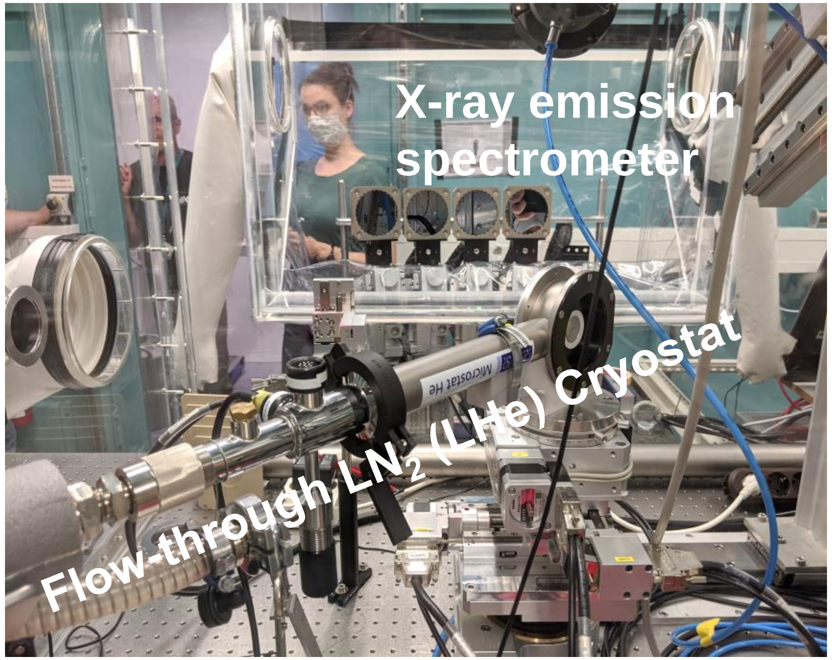

Zimina, A. et al. Review of Scientific Instruments 88, 113113 (2017)
Schacherl, B. et al. Anal. Chim. Acta 2022, 1202, 339636.
Schacherl, B. et al. J. Synchrotron Radiat. 2022, 29 (1), 80–88.

Motivation: The mechanism of Fe induced bond stability of uranyl(V)

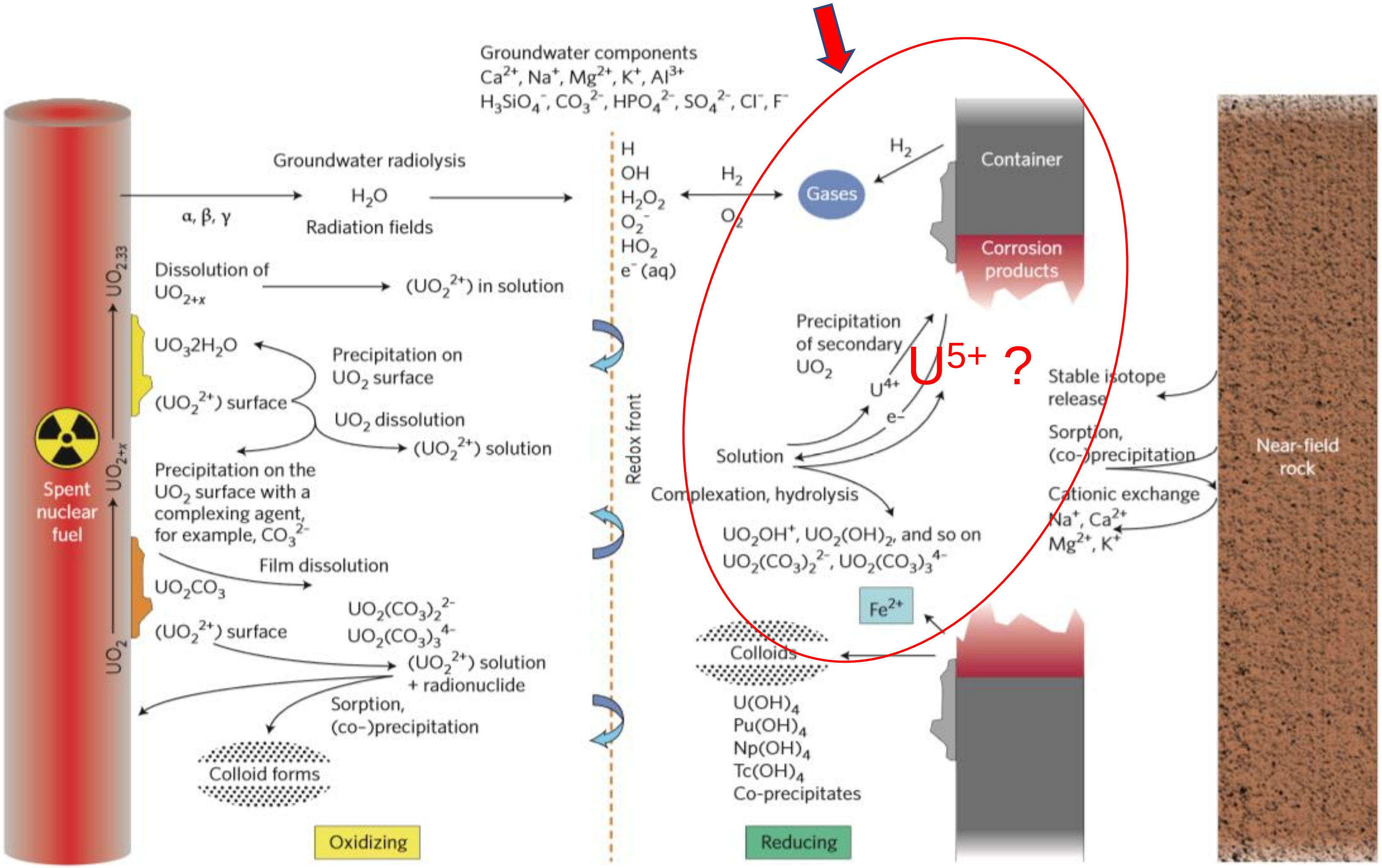

R. Ewing, Nature Mat., 2015

Oxidation state investigations applying U M_4 edge HR-XANES

U L_3 edge XANES

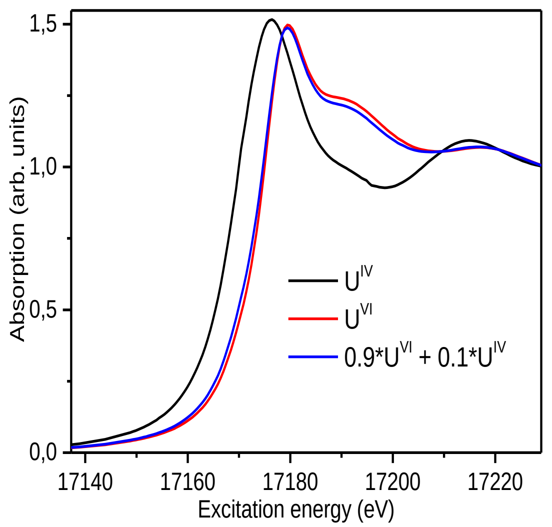

U L_3 edge HR-XANES

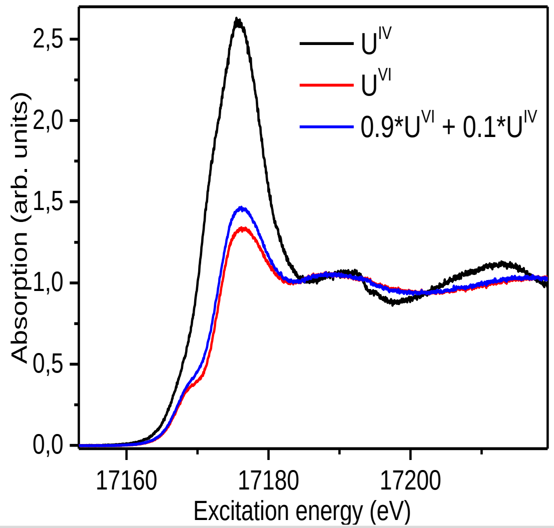

U L_3 or U M_4 HR-XANES is more sensitive to U oxidation states?

U M_4 edge HR-XANES

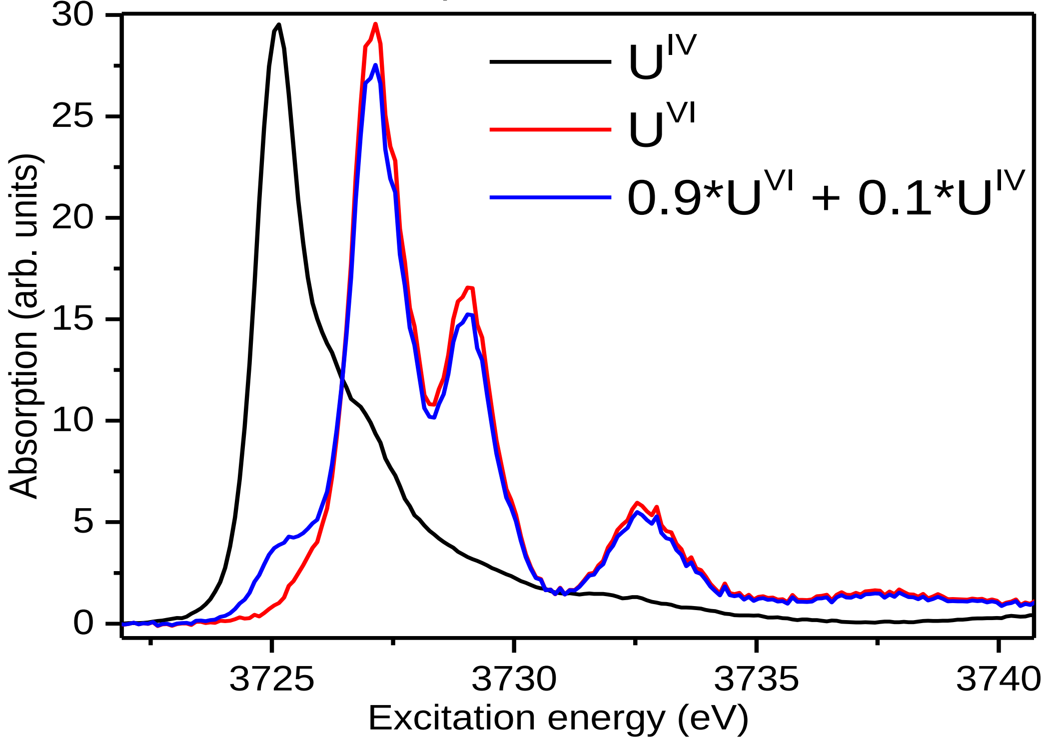

The mechanism of Fe induced bond stability of uranyl(V)

U L_3 edge HR-XANES   U M_4 edge HR-XANES

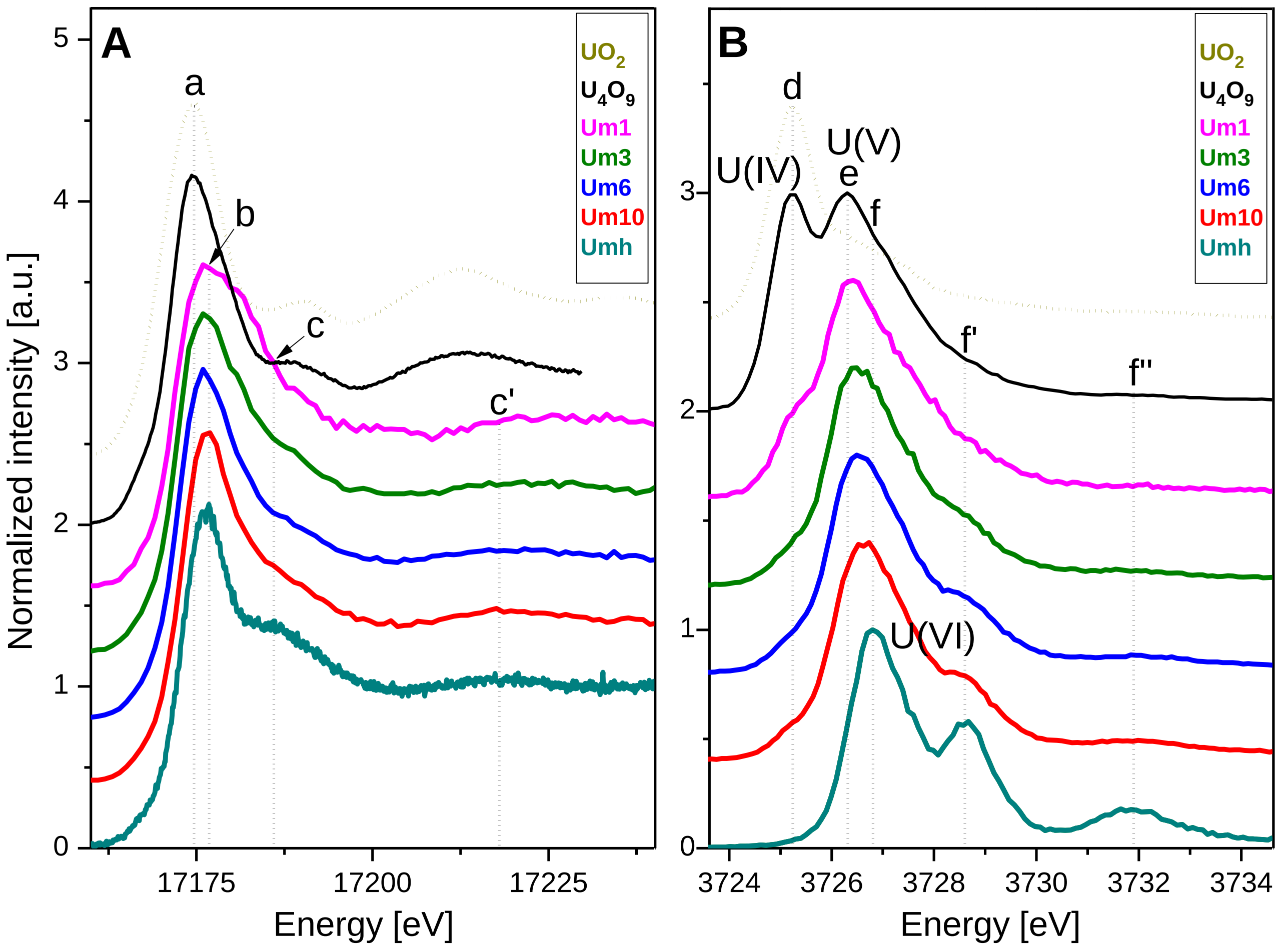

Only U M_4 HR-XANES detects:

- **U^{IV}, U^{V} and U^{VI} in the same sample**

I. Pidchenko et al., Environmental Science & Technology. 51 (2017) 2217

The mechanism of Fe induced bond stability of uranyl(V)

U(V)-O-Fe incorporated in magnetite “long term” stable even in air => Why?

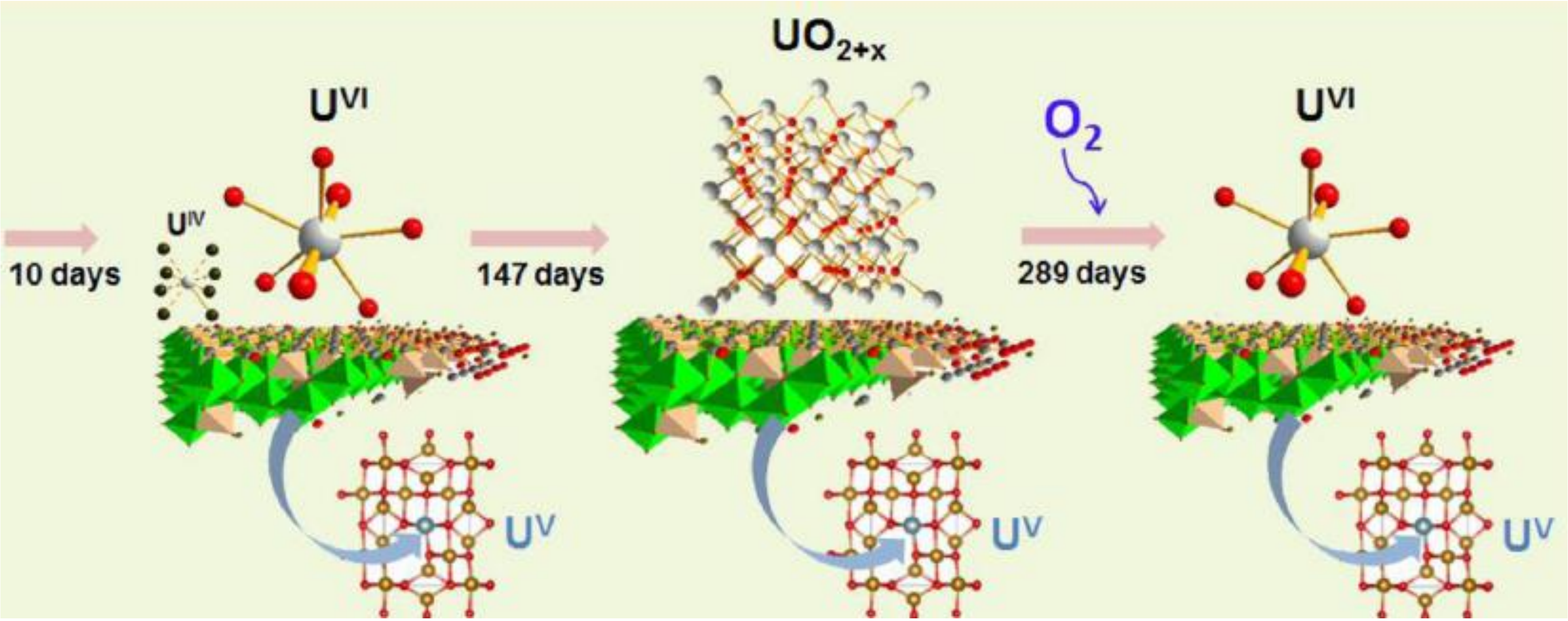

I. Pidchenko et al., Environmental Science & Technology. 51 (2017) 2217

The mechanism of Fe induced bond stability of uranyl(V)

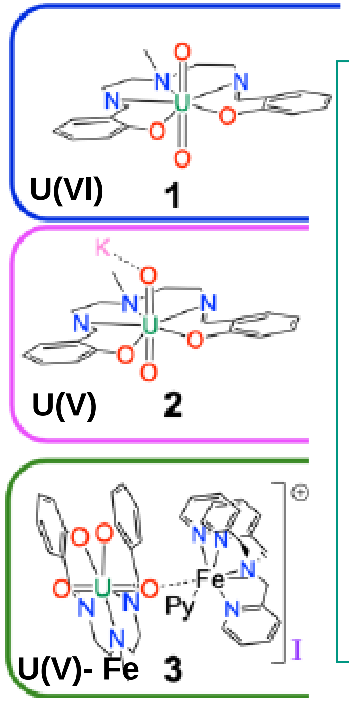

Ligand: Mesaldien^{2-}

R. Faizova et al. *Chem Sci* 9 (2018) 7520:

Fe(II) stabilises U(V)-yl against proton induced disproportionation

Cyclic voltammetry: increased range of stability of U(V) + Fe(II)

T. Vitova, L. Maron, M. Mazzanti et al., Chem. Sci. 13 (2022) 11038

U M_4 HR-XANES of actinyls:
Tool for detection changes of U-Oax bond covalency

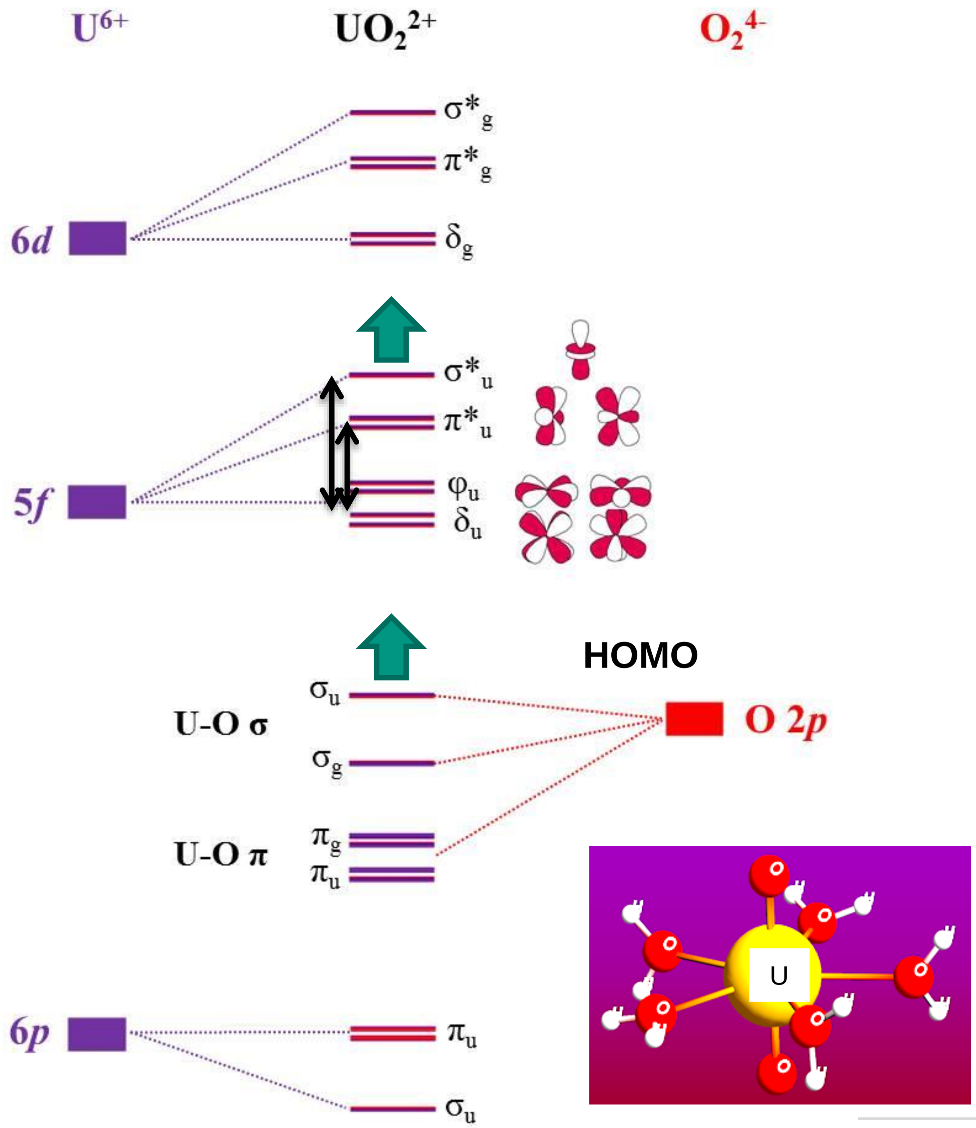

„Pushing from below“

- Large energy shift of 5*fσ** compared to 5*fδ*/*ϕ* => Large An-Oax bond covalency

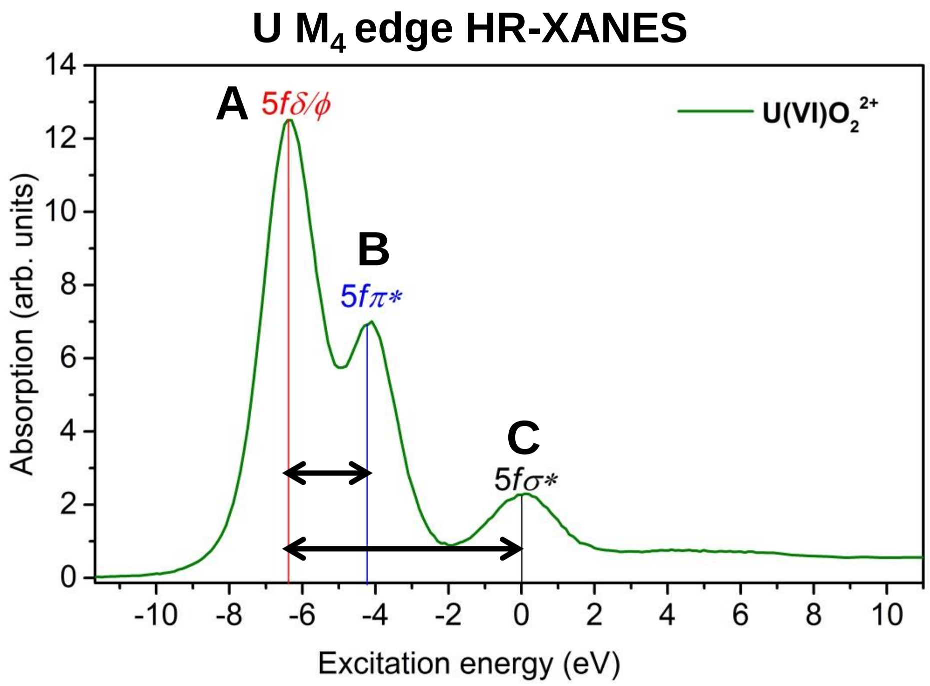

T. Vitova et al., Nature Communications 8 (2017) 16053

U $M_{4,}$ edge valence band resonant inelastic X-ray scattering (VB-RIXS): Tool for detection of U-ligands bond covalency

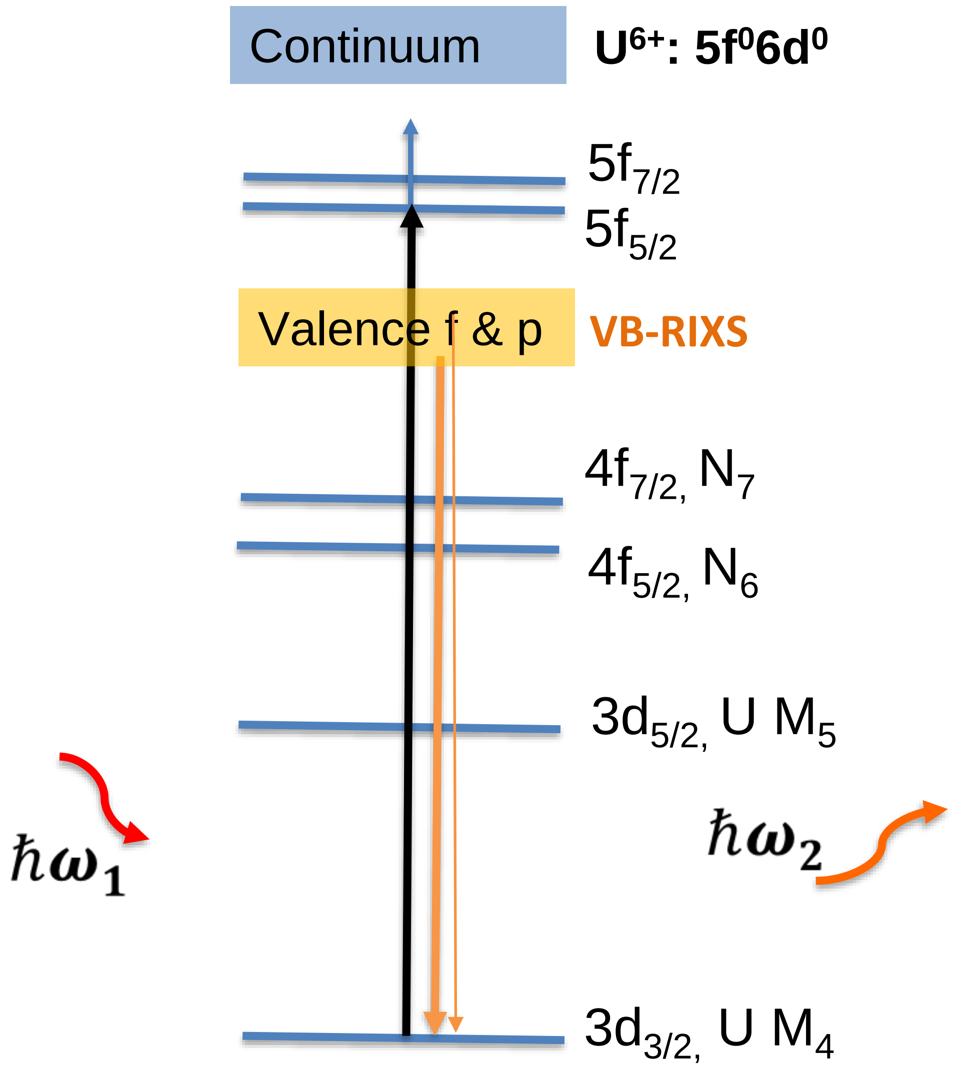

- Large area => Large U 5f contribution to the valence band
  => Large U-ligands bond covalency

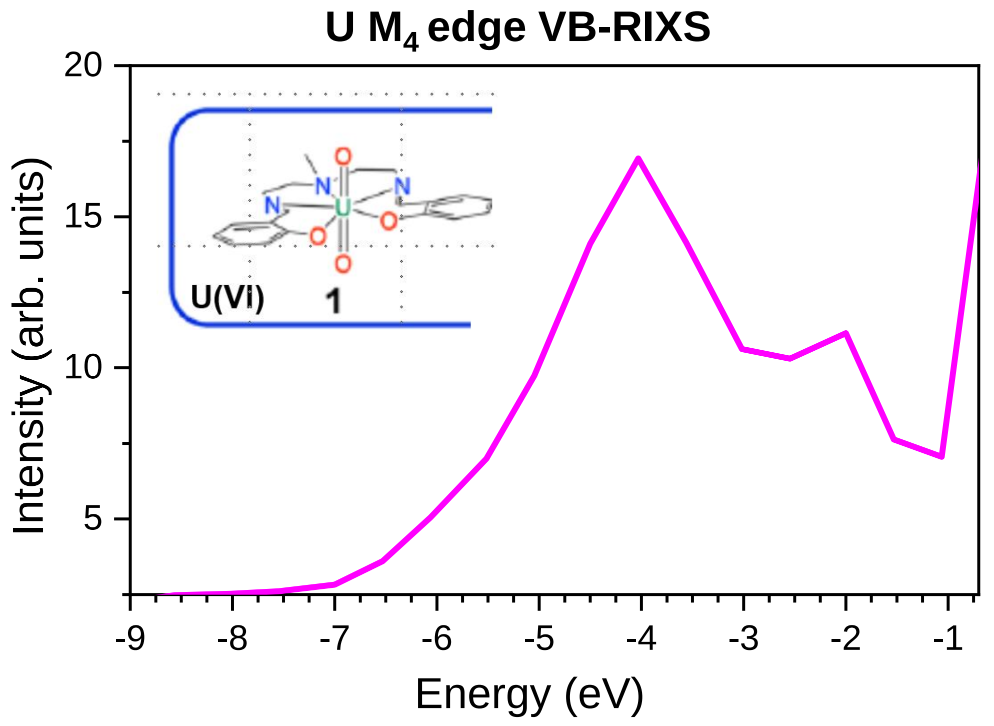

T. Vitova, L. Maron, M. Mazzanti et al., Chem. Sci. 13 (2022) 11038

The mechanism of Fe induced bond stability of uranyl(V)

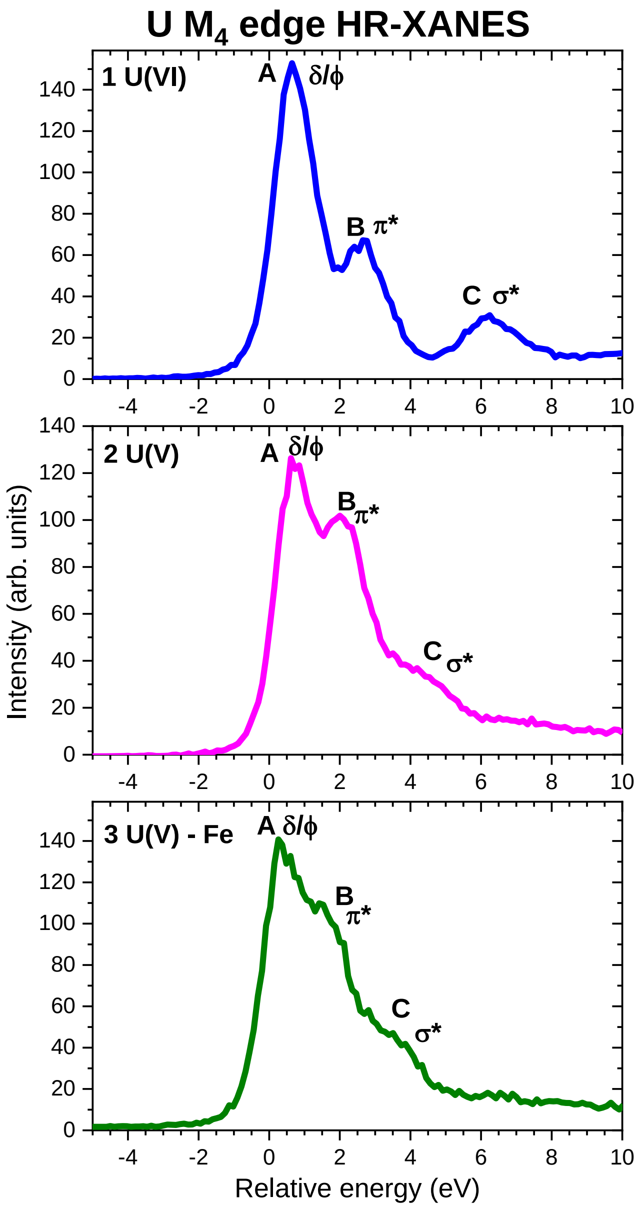

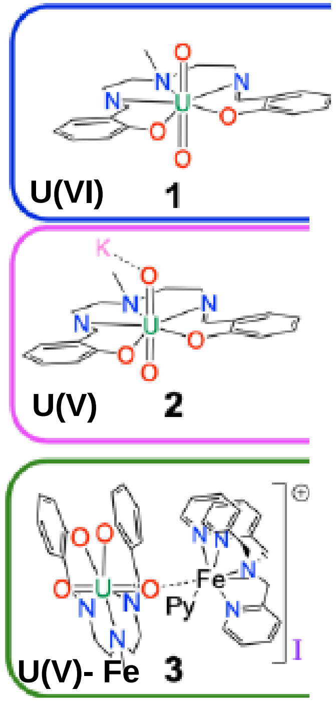

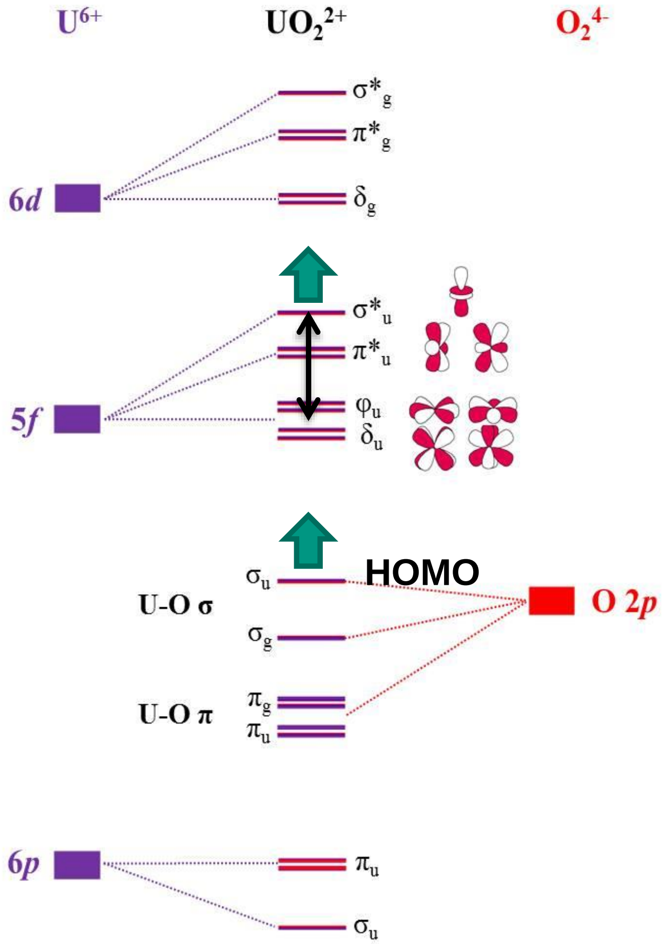

T. Vitova, L. Maron, M. Mazzanti et al., Chem. Sci. 13 (2022) 11038

The mechanism of Fe induced bond stability of uranyl(V)

U-Oax
bond covalency decreases
U(VI)>U(V)>U(V)-Fe

DFT (NBO, WBI bond analyses) supports the experimental results

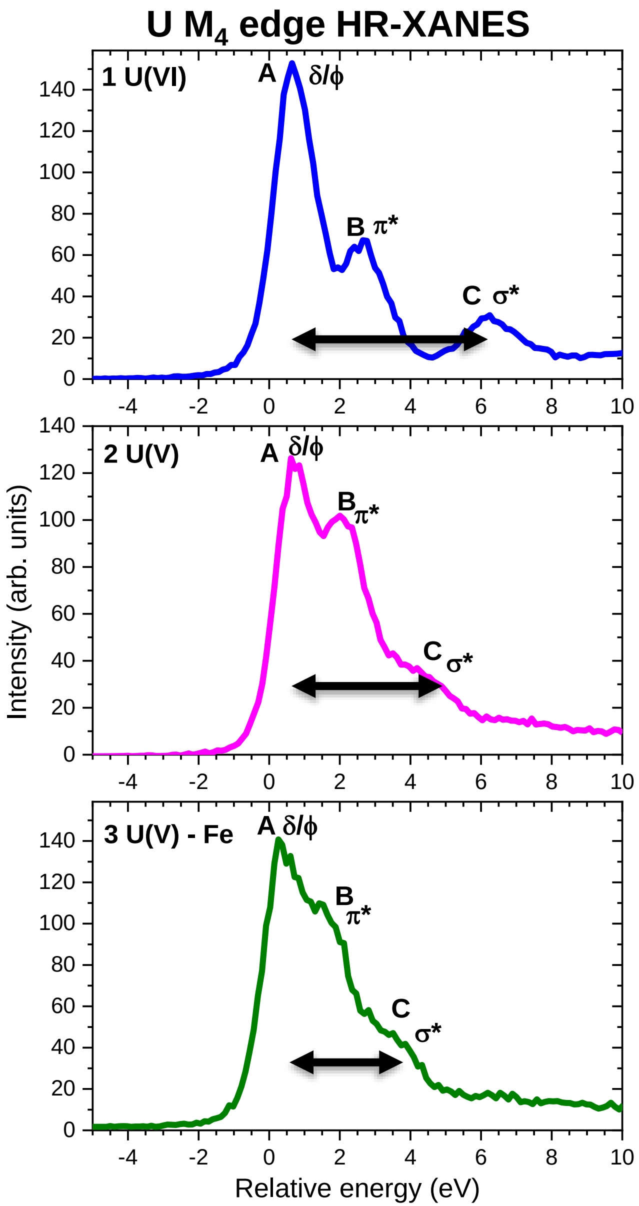

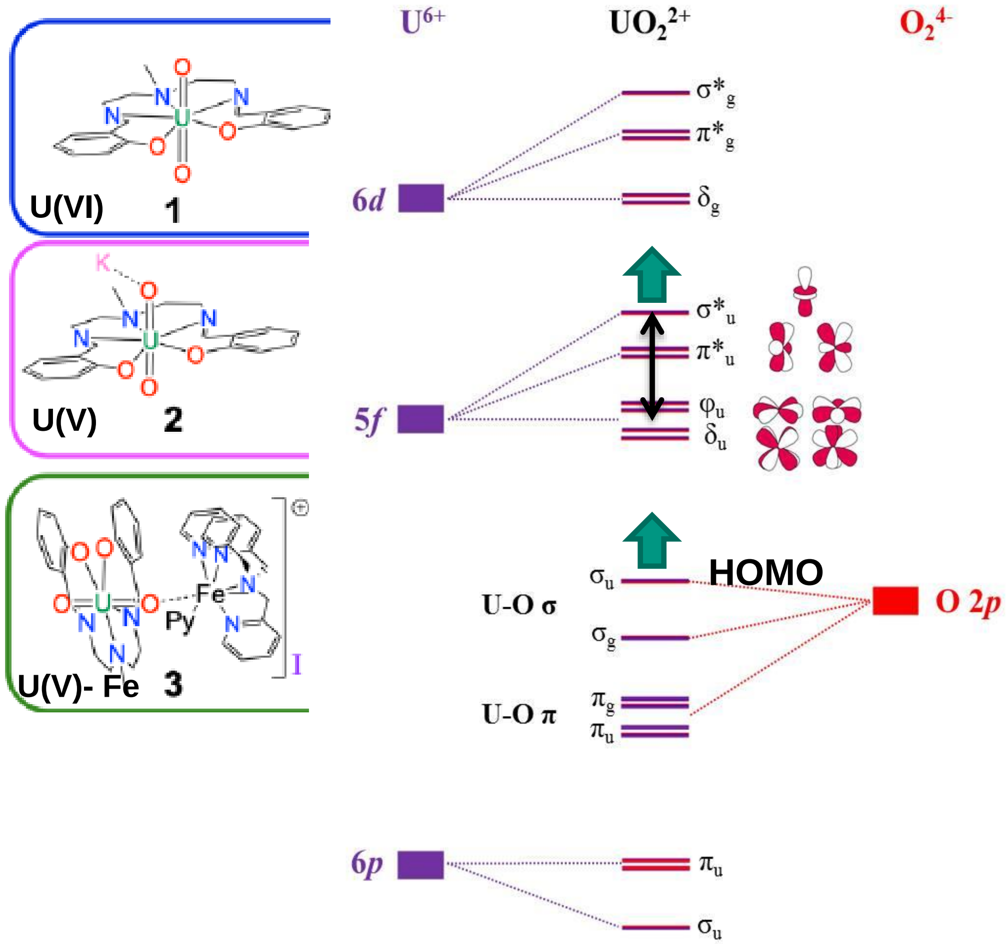

T. Vitova, L. Maron, M. Mazzanti et al., Chem. Sci. 13 (2022) 11038

The mechanism of Fe induced bond stability of uranyl(V)

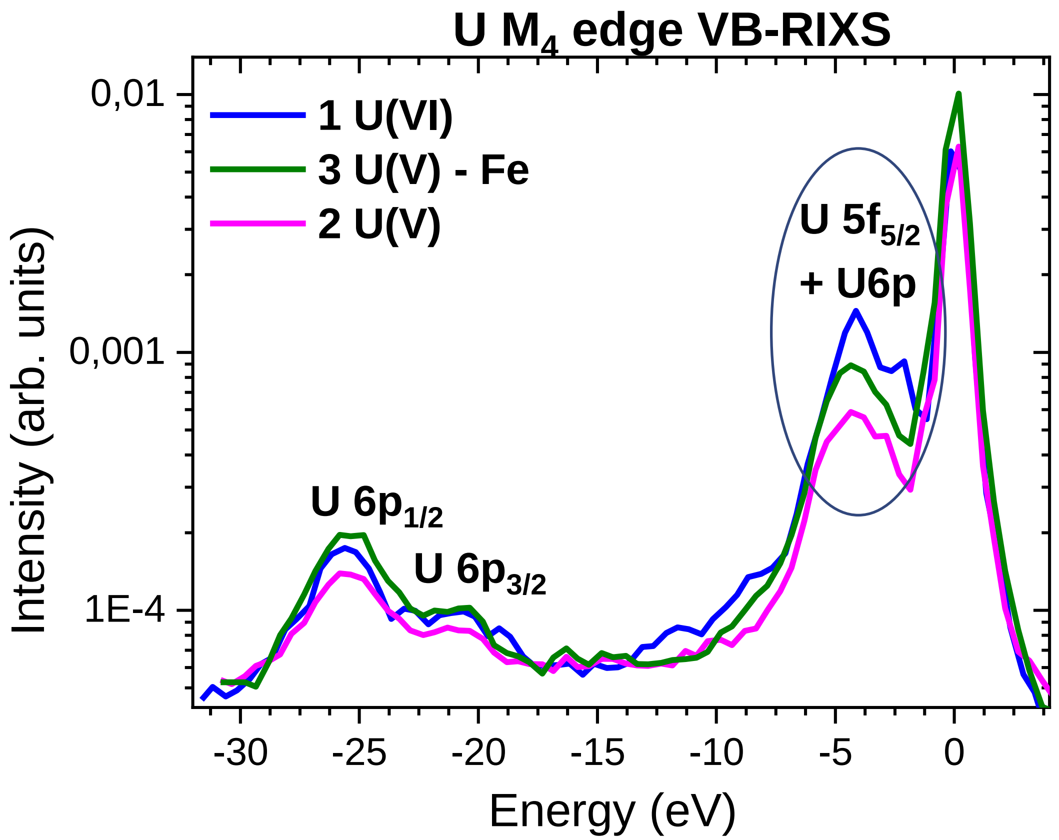

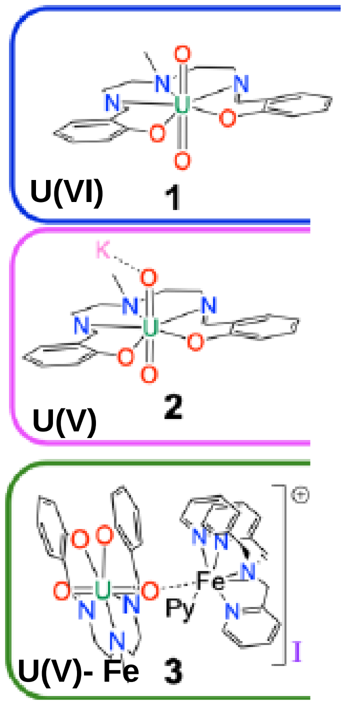

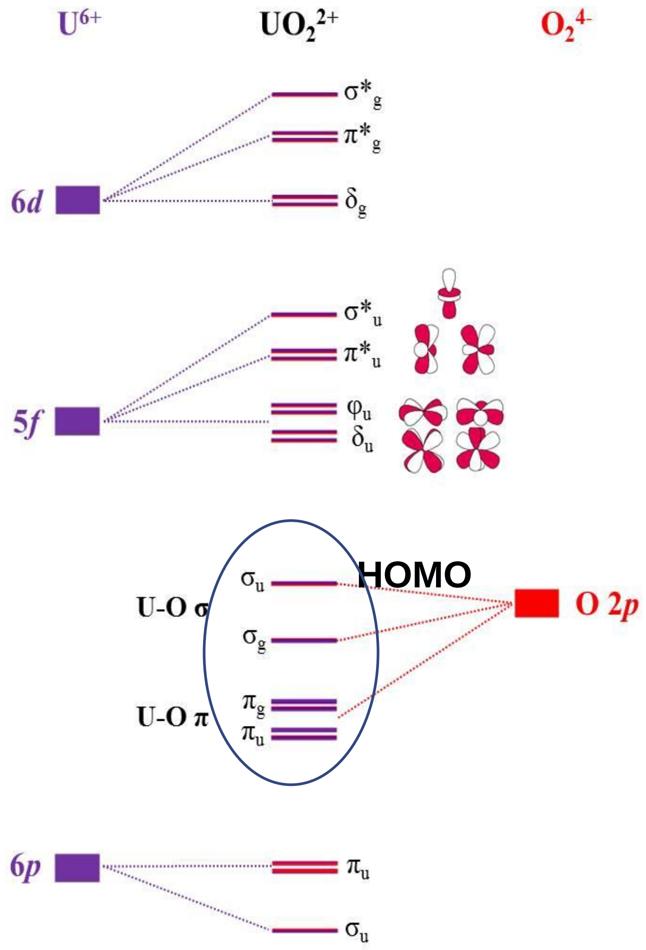

U-ligands bond covalency decreases U(VI)>U(V)-Fe>U(V)

DFT (NBO, WBI bond analyses) supports the experimental results

T. Vitova, L. Maron, M. Mazzanti et al., Chem. Sci. 13 (2022) 11038

Stabilisation of U(V)-yl by Fe(II)

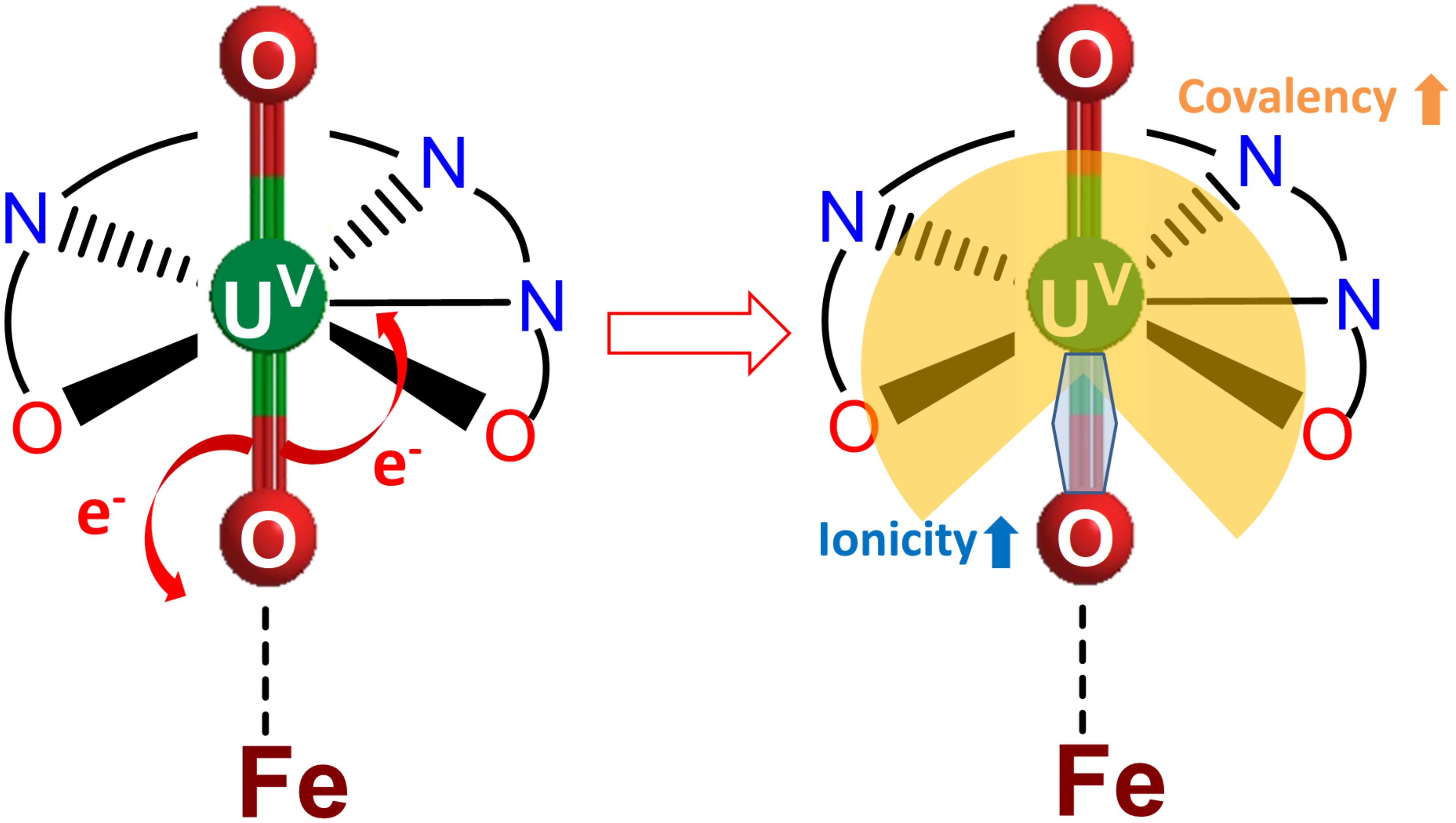

T. Vitova, L. Maron, M. Mazzanti et al., Chem. Sci. 13 (2022) 11038

Understanding radionuclide - mineral surface redox reactions

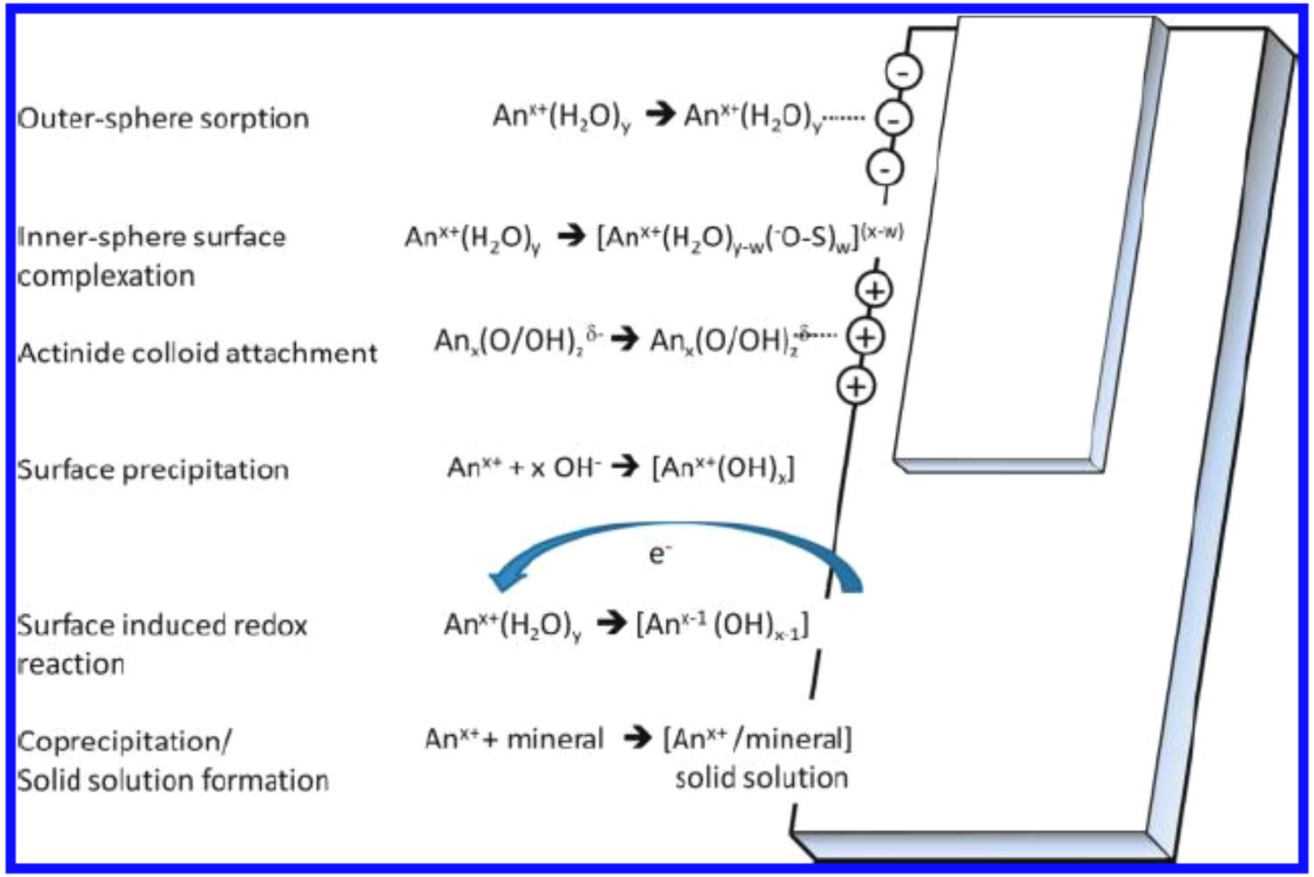

H. Geckeis et al. Chem Rev 113, (2013) 1016-62

Karlsruhe Institute of Technology

Challenges:

- **An L_3 edge XANES low sensitivity to mixtures of oxidation states**
- **An concentrations above solubility limit are mostly studied**
- **Radiation damage**

Solution:

- **An $M_{4,5}$ edge HR-XANES at cryogenic temperatures**

Too high An concentrations often needed for XAS/XANES

Karlsruhe Institute of Technology

(1)

Add more ^{237}Np

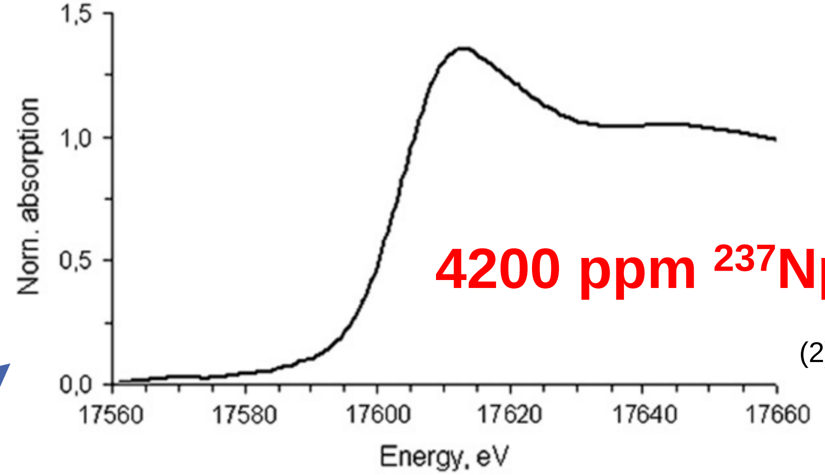

(2)

Np sorbed on clay mineral illite

3 - 95 ppm ^{237}Np

Add more ^{237}Np

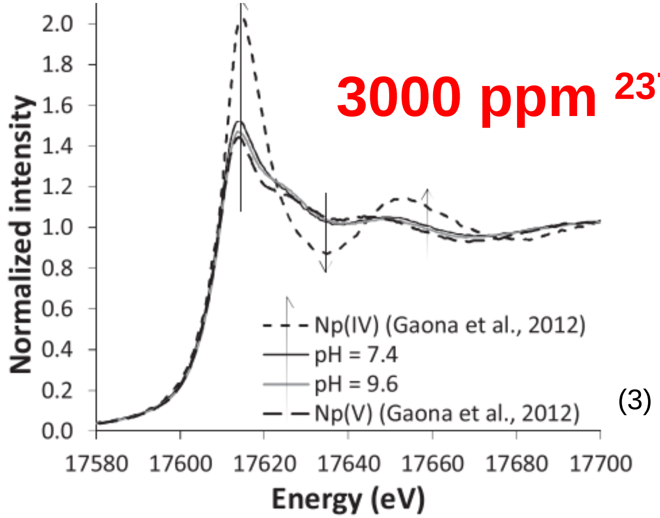

(3)

(1) https://www.orangesmile.com/extreme/en/radioactive-zones/mayak-factory.htm#object-gallery accessed 01.12.2022
(2) Kalmykov, S. N. et al. *Comptes Rendus Chim.* 2007, *10* (10–11), 1060–1066.
(3) Marsac, R. et al. *Geochim. Cosmochim. Acta* 2015, *152*, 39–51.

1ppm Np detection limit at the Np M_5-edge HR-XANES

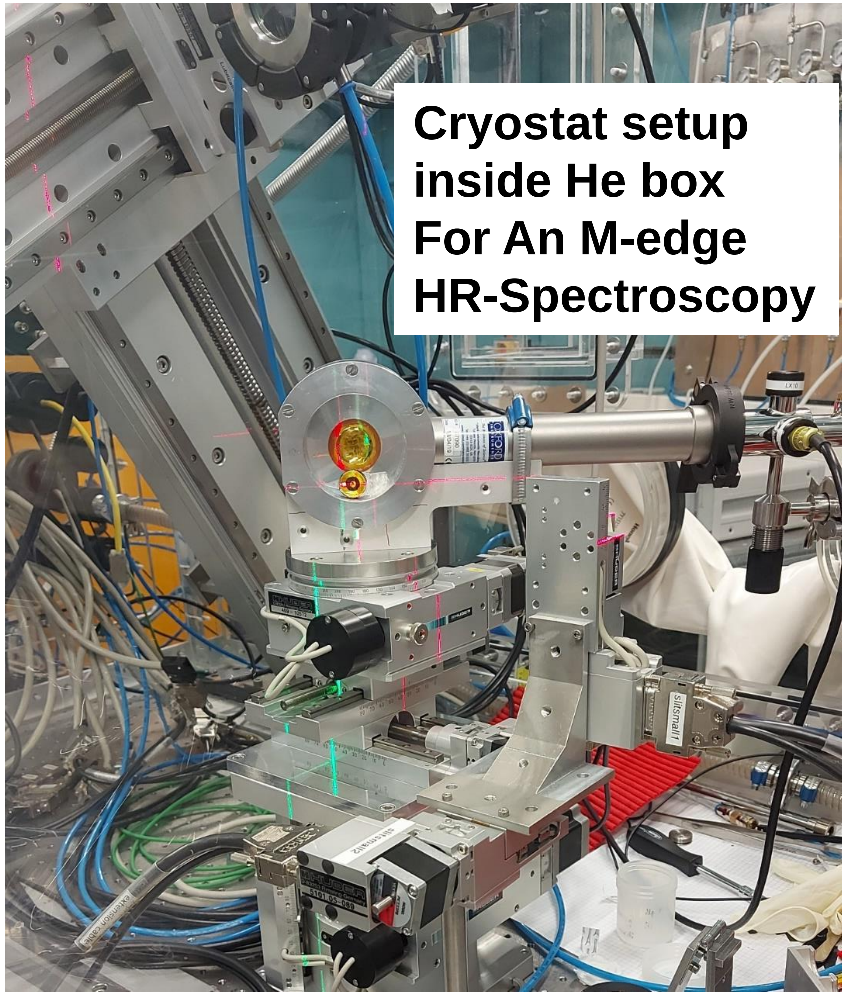

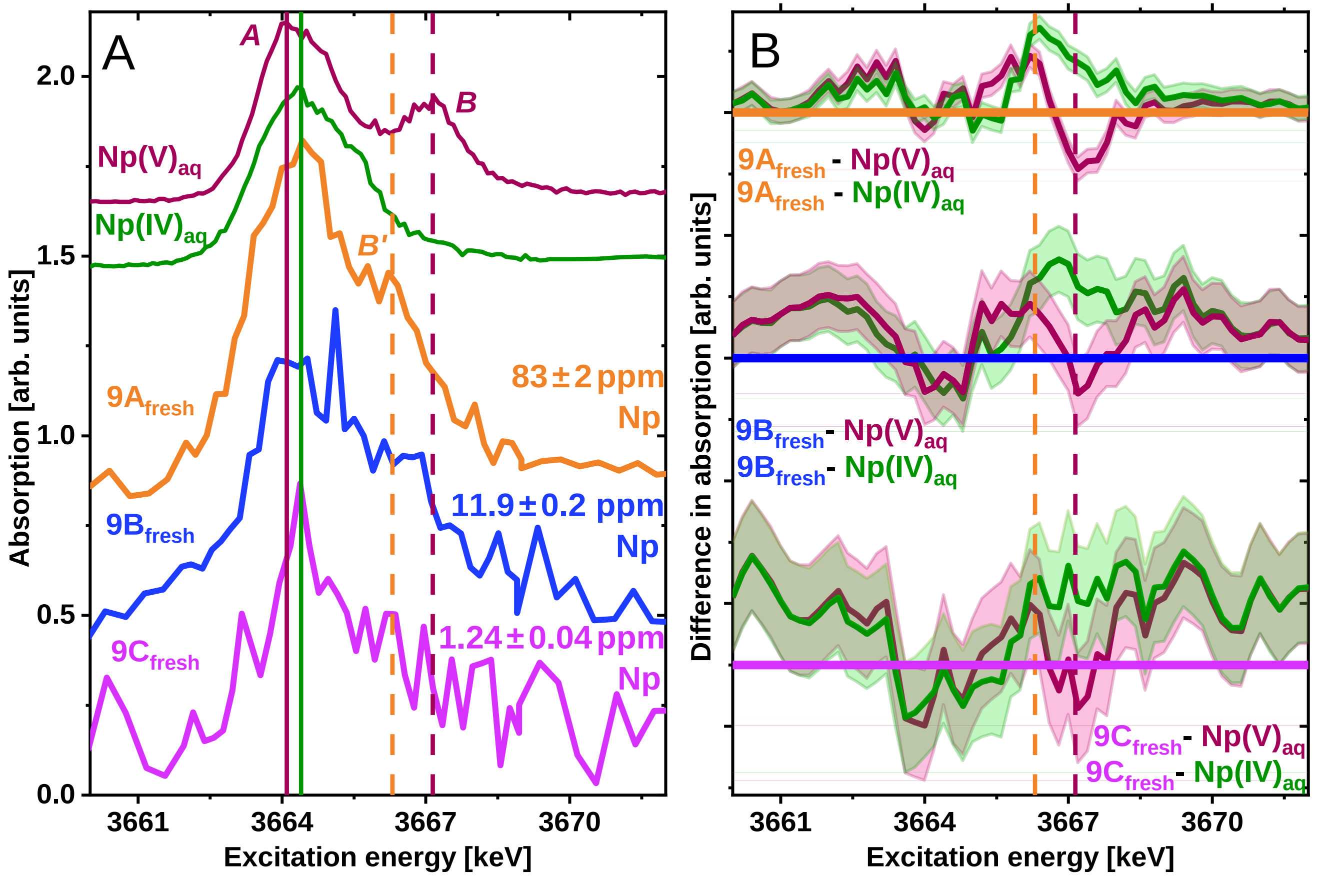

Schacherl, B. et al. J. Synchrotron Radiat., (2022) 29, 80-88; Anal. Chim. Acta (2022) 1202, 339636; Environ. Sci. Technol., (2023) 57, 30, 11185

Motivation: Understanding aging and corrosion of spent nuclear fuel (SNF)

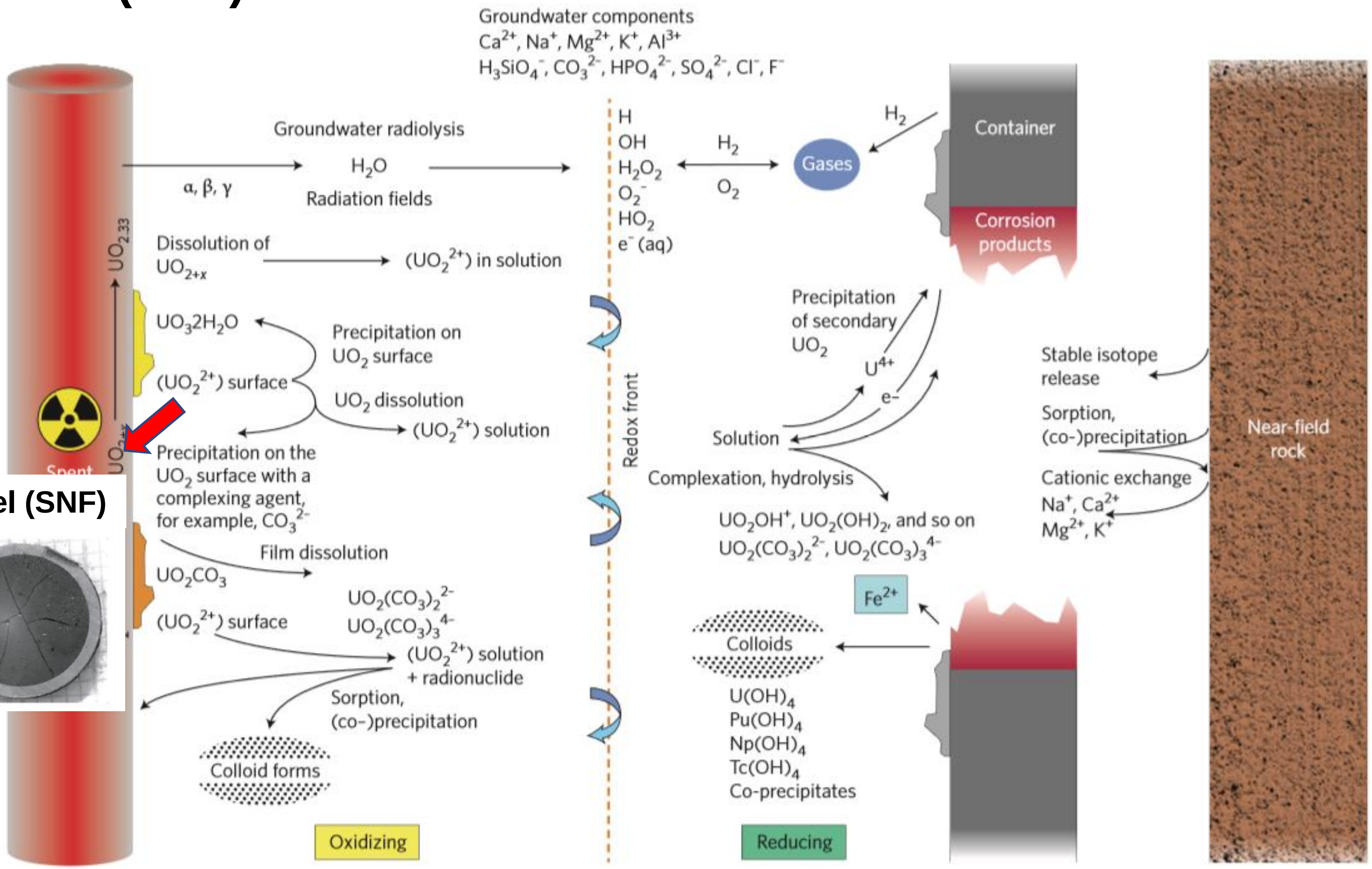

Spent Nuclear Fuel (SNF)

R. Ewing, Nature Mat., 2015

Motivation: Understanding aging and corrosion of spent nuclear fuel (SNF)

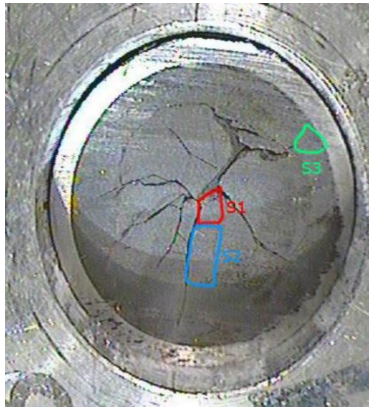

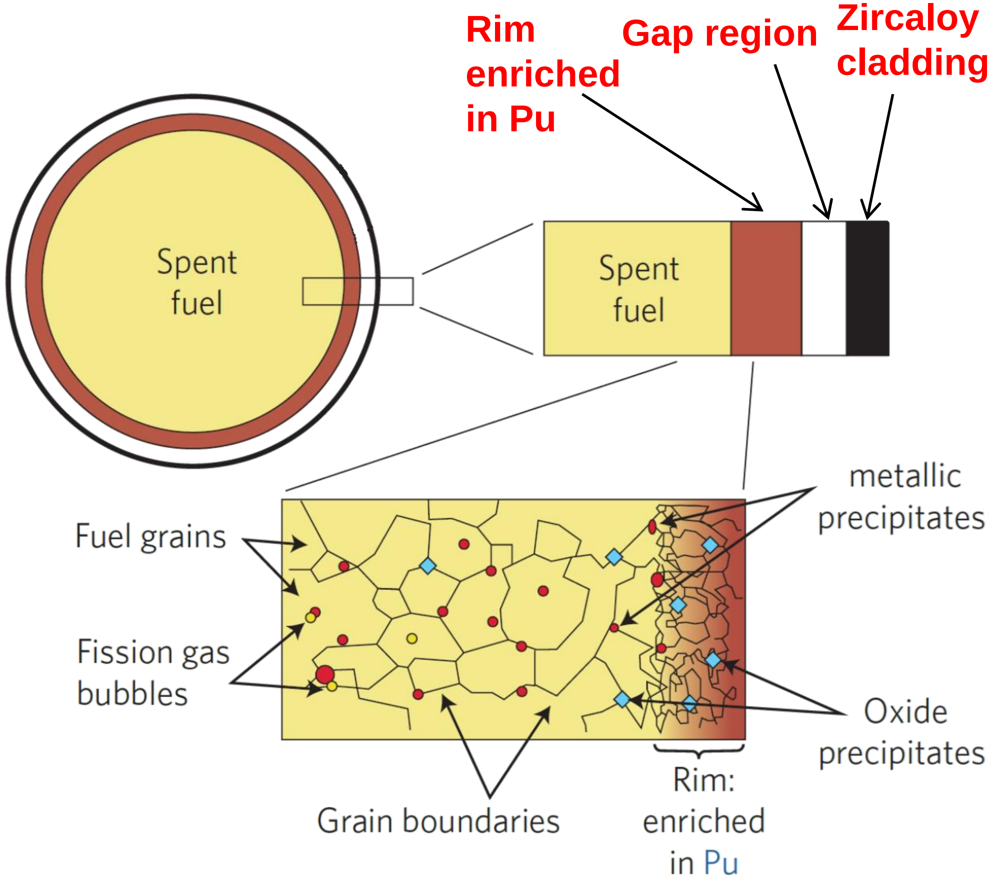

The SNF waste package is a complex system

(1) Changes of redox states of U/Am from center to rim of a SNF pellet?

(2) U redox state in the SNF/Zircaloy interface?

Particles from the center to the rim of the SNF pellet

- S1: central particle
- S2: midway particle
- S3: periphery
- S4: cladding, inner surface

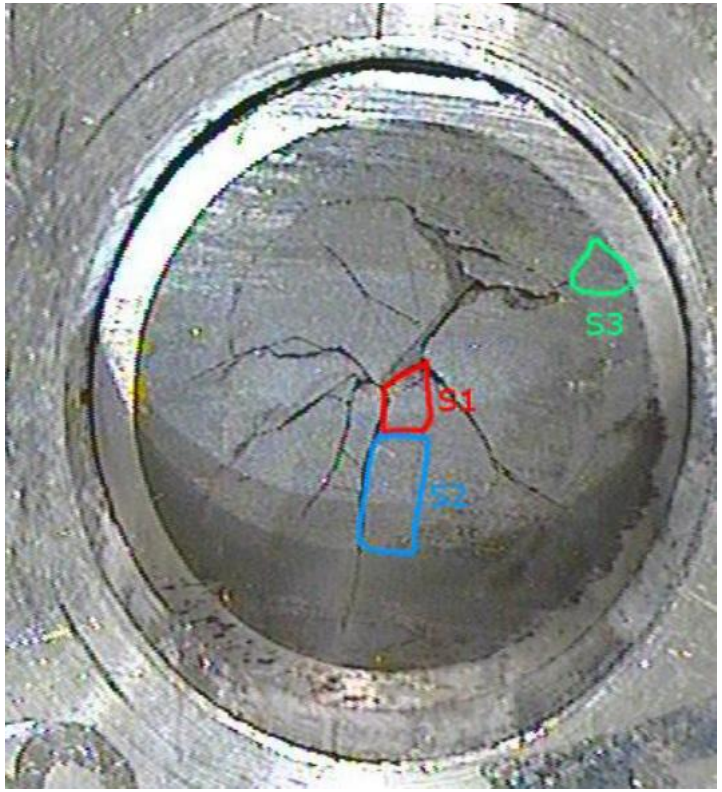

A. Bulgheroni et al., JRC Internal Report 2018, PUBSY No. JRC114106

Particles from the center to the rim of the SNF pellet

S1: central particle
S2: midway particle
S3: periphery
S4: cladding, inner surface

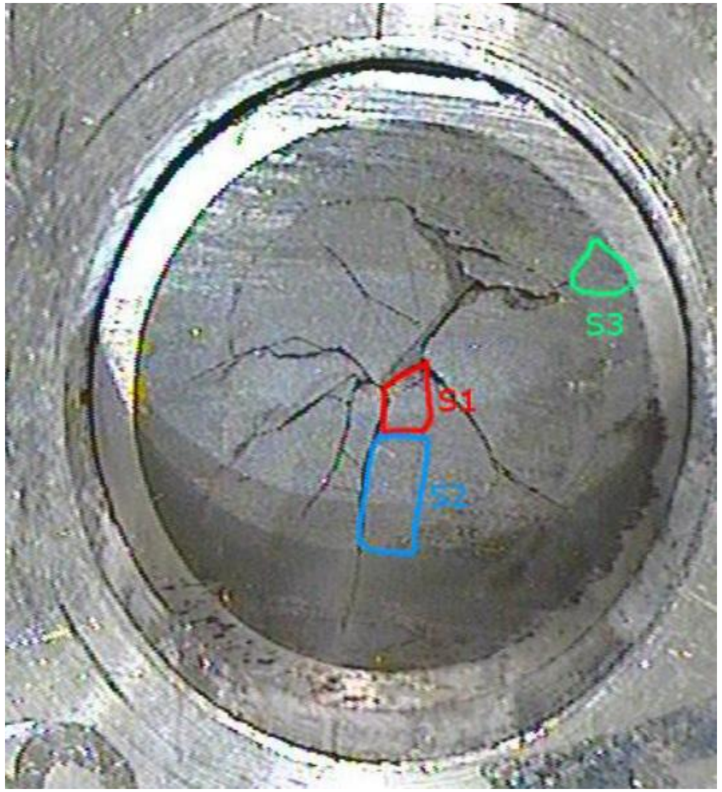

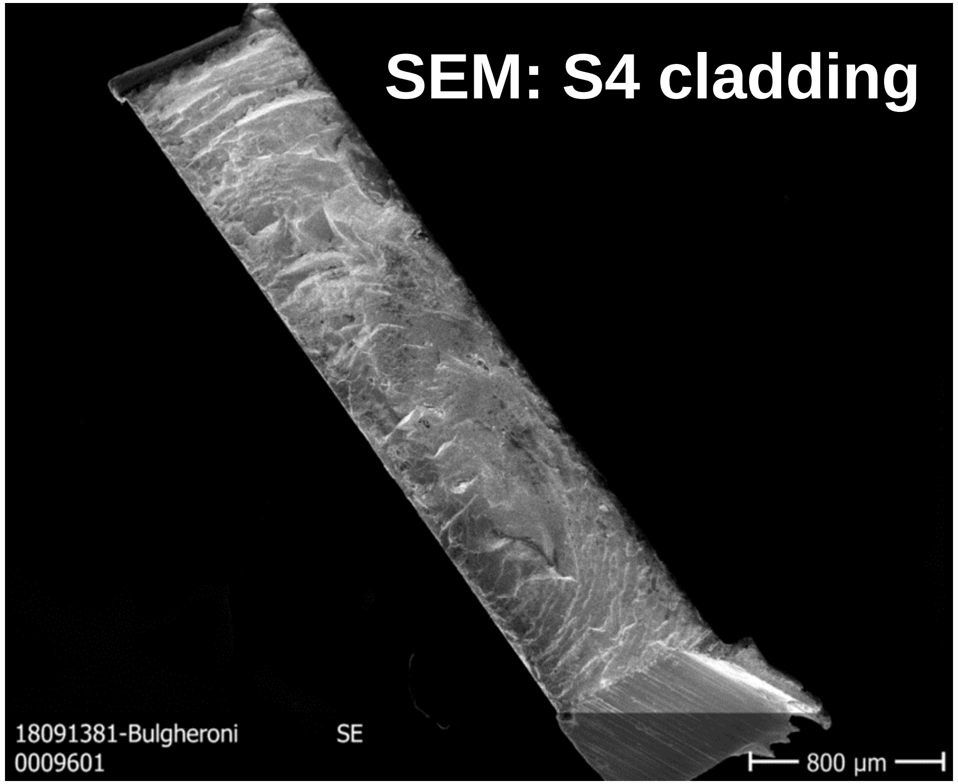

A. Bulgheroni et al., JRC Internal Report 2018, PUBSY No. JRC114106

Changes of redox state of U from the center to the rim of the SNF pellet

U Mβ fluorescence maps

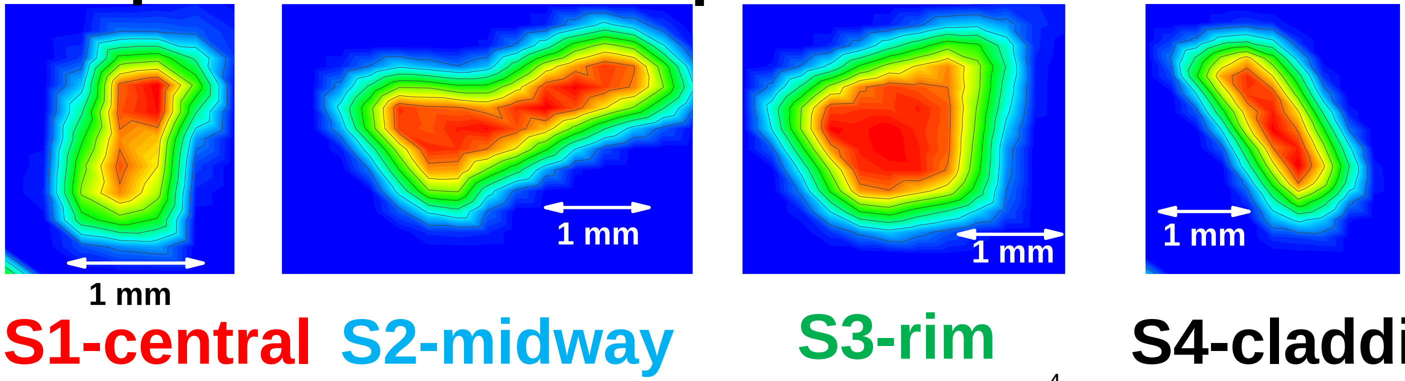

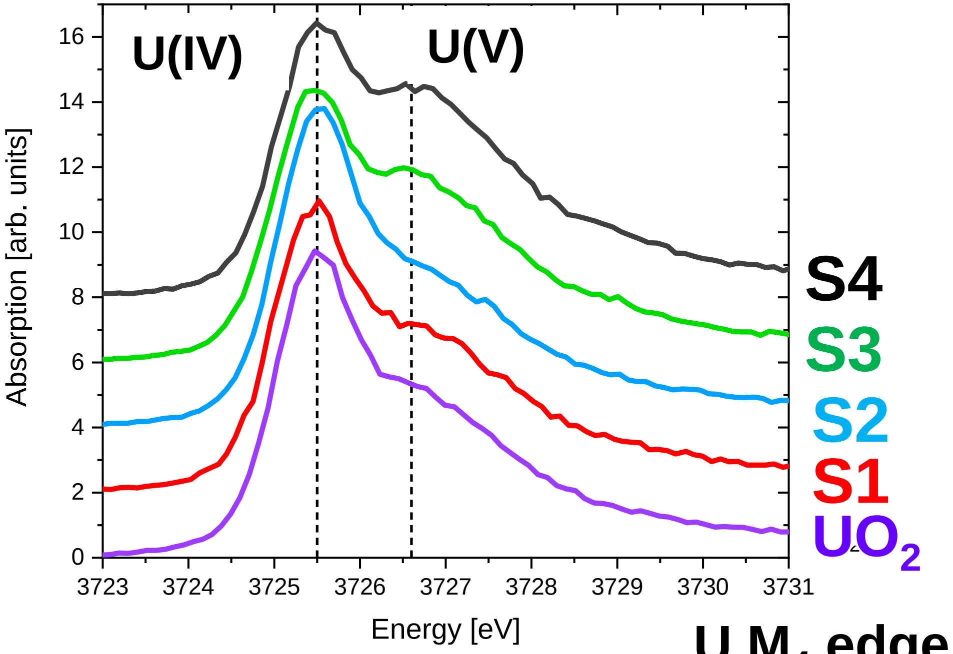

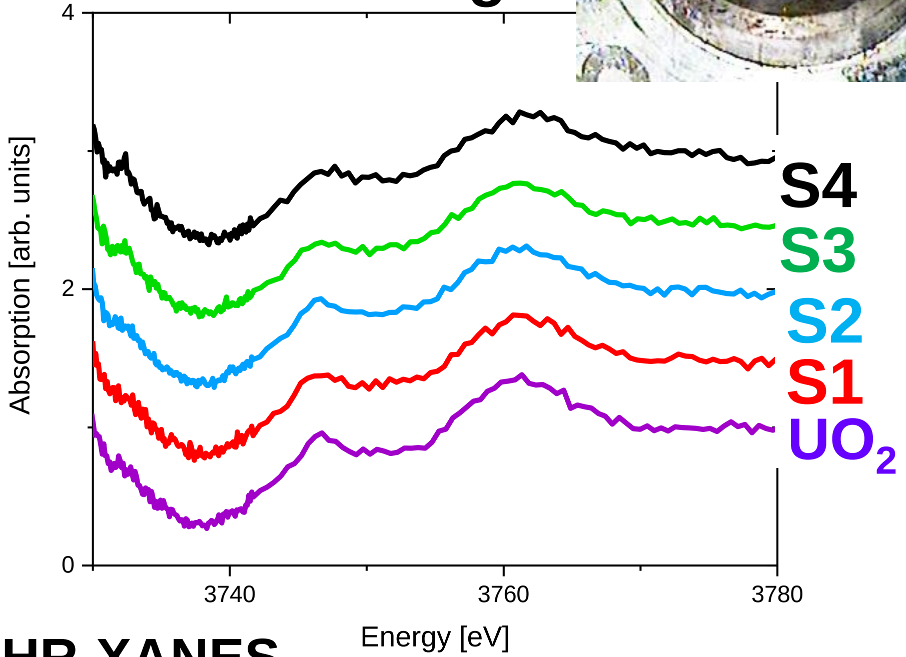

U M_4 edge HR-XANES

Morphology of SNF

Core region of a SNF pellet

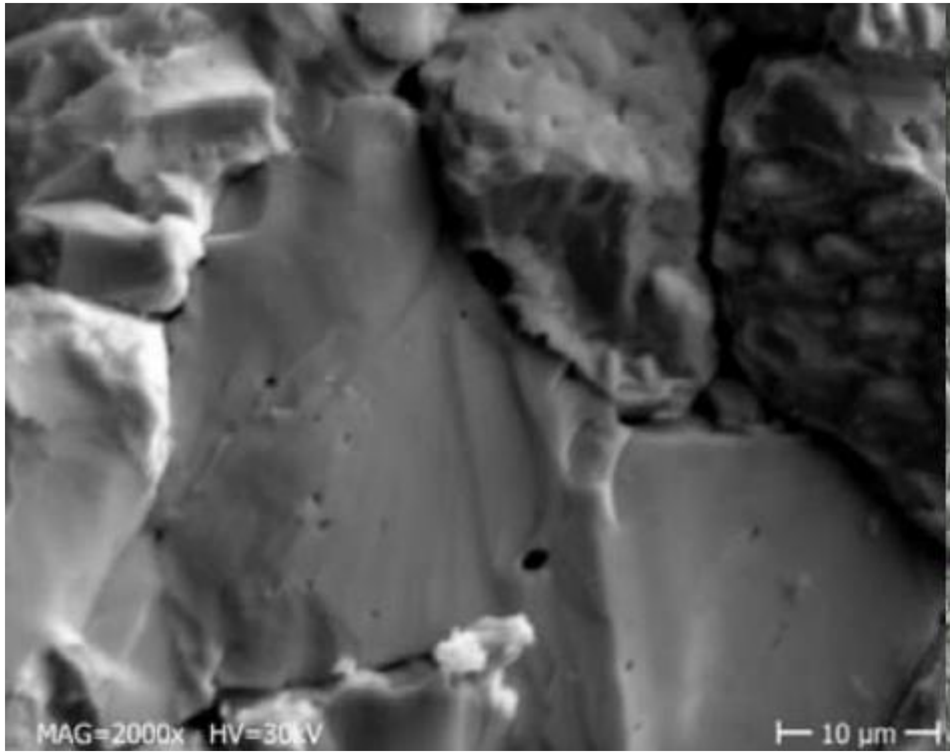

Rim region of a SNF pellet

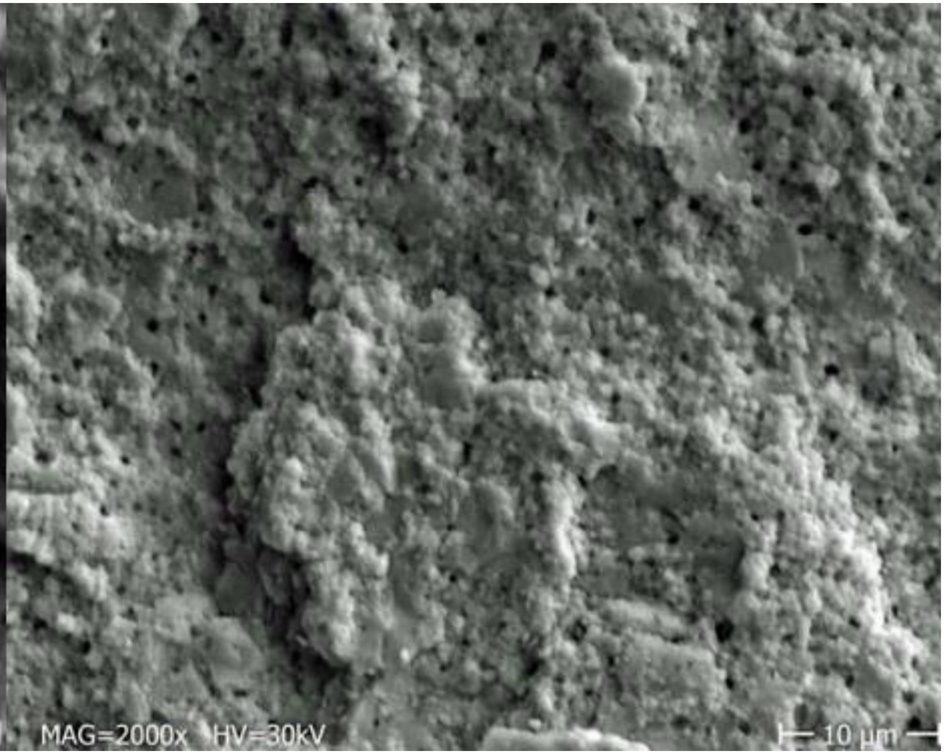

D. H. Wegen, S. Bremier and D. Pellottiero, SEM Study on High Burn-up Fuel - JRC104732, 2016.

Morphology of SNF

Possible charge compensation mechanism: surface oxidation U(IV) ⇨ U(V)

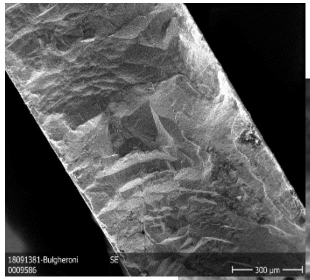

S4 SNF – Cladding

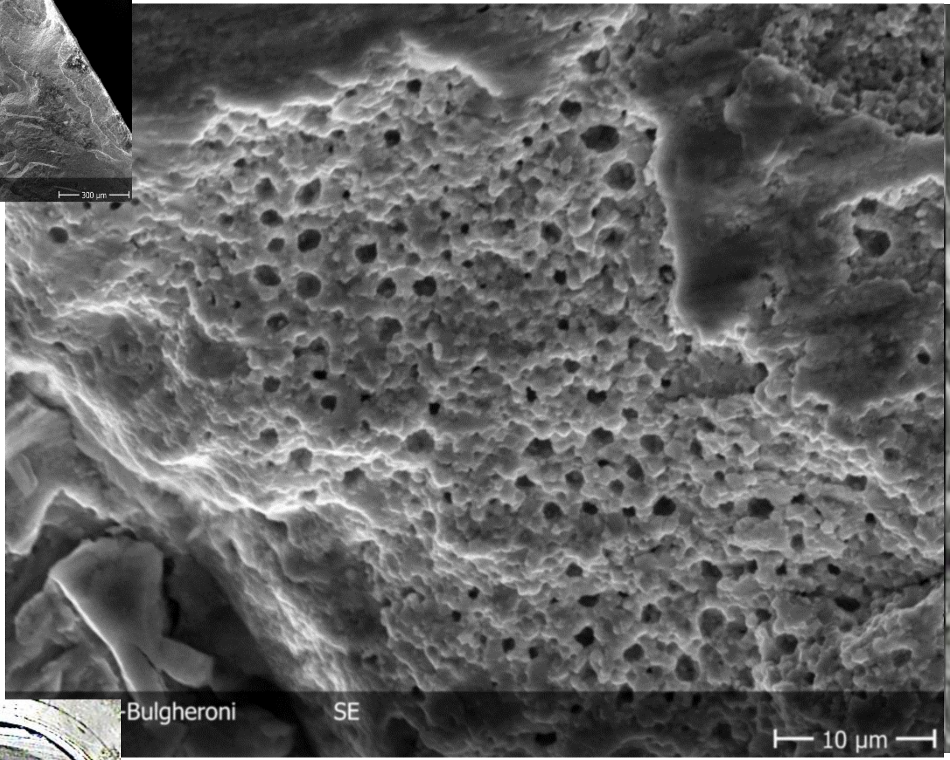

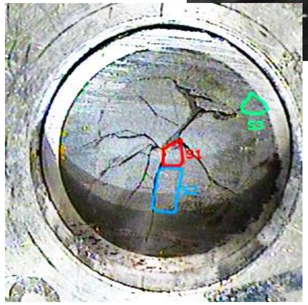

Rim region of a SNF pellet

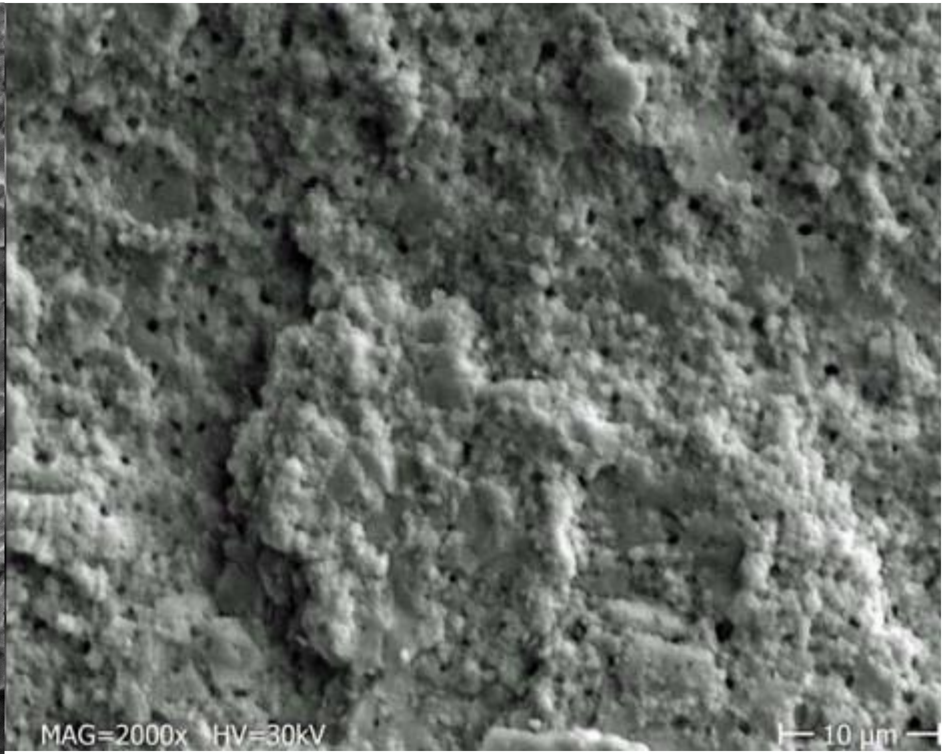

D. H. Wegen, S. Bremier and D. Pellottiero, SEM Study on High Burn-up Fuel - JRC104732, 2016.

Changes of redox state of Am from the centre to the rim of the pellet

Possible charge compensation mechanism:
U(IV) ➡ U(V) & Am(IV) ➡ Am(III)

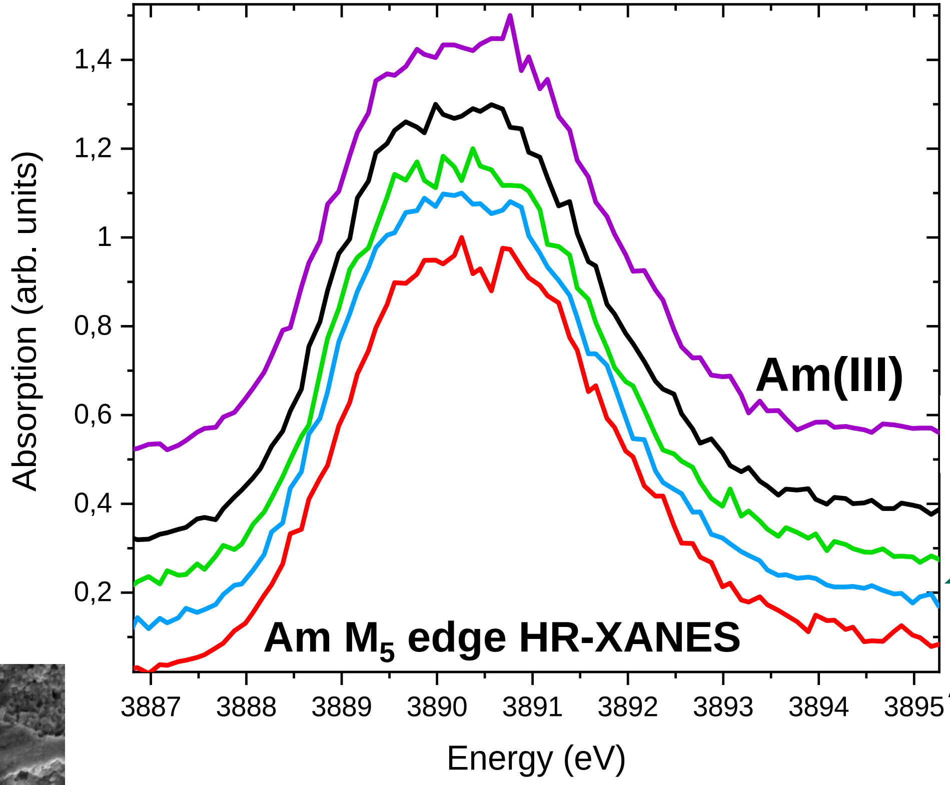

Am(III), U(V)

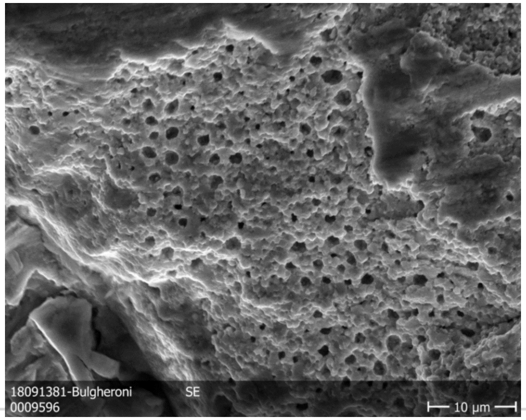

E. Epifano et al.,Communications Chemistry 2 (2019) 59

How stable are nanosized AnO_2 compounds against oxidation?

Charge compensation mechanism:
U(V) ➡ U(IV)

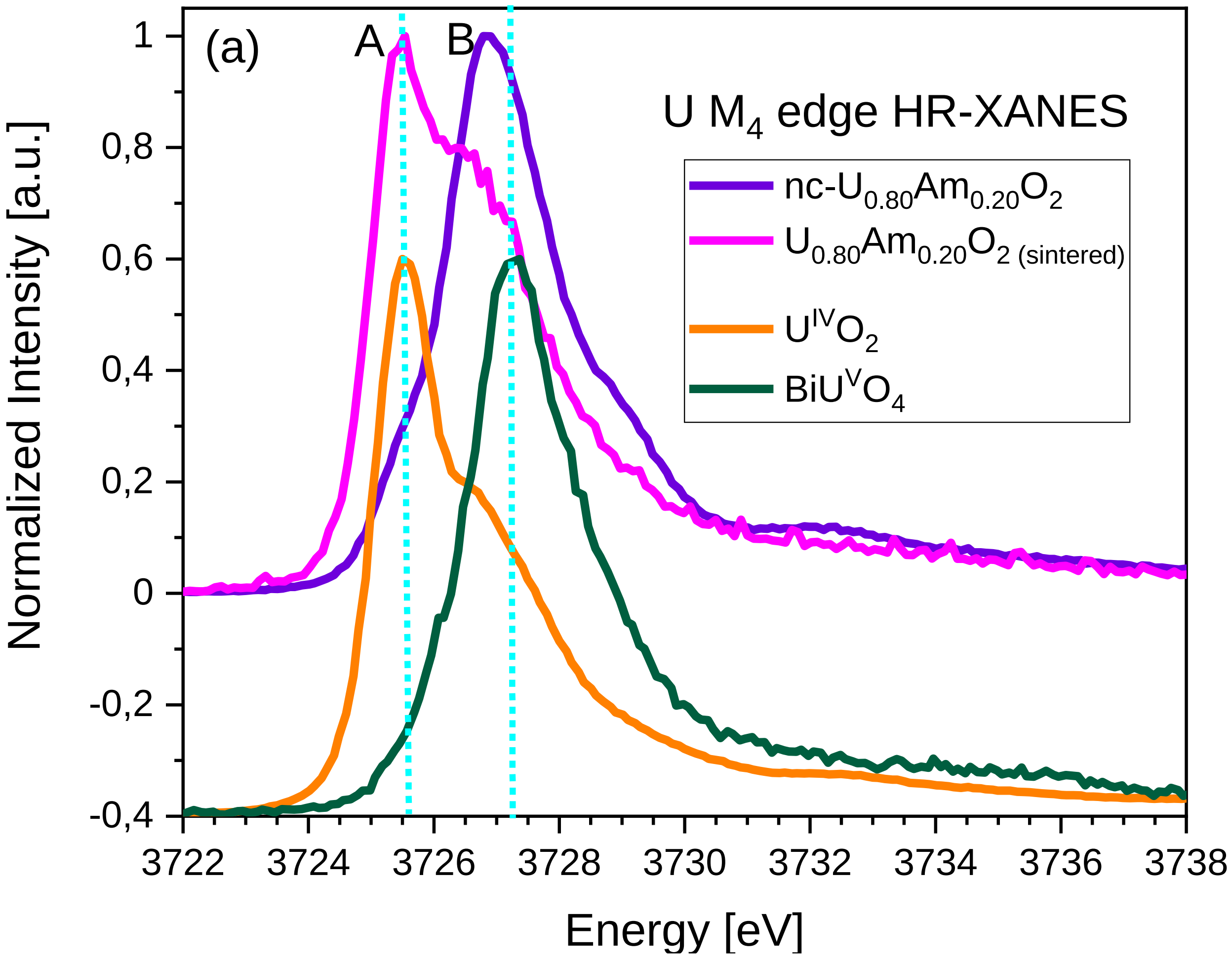

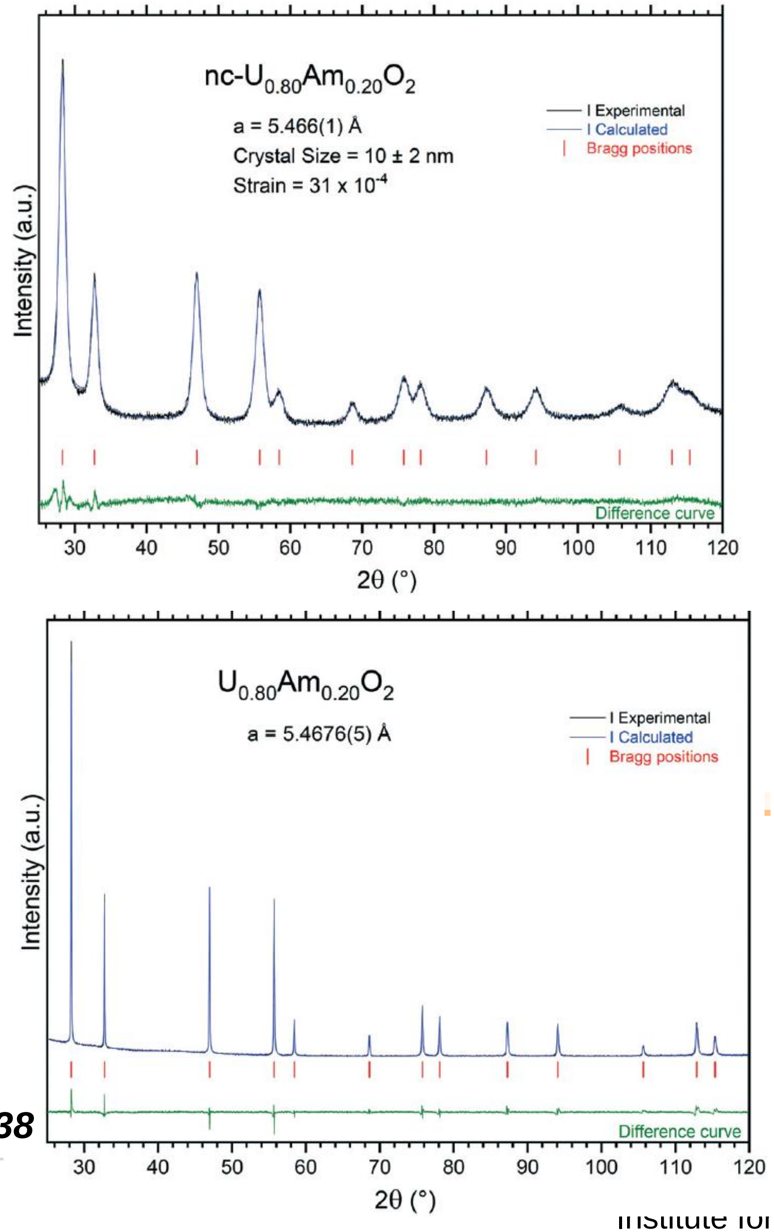

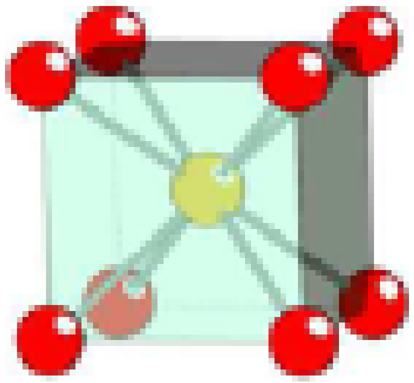

J.F. Vigier, O. Walter, T.Vitova, K. Popa et al. CrystEngComm, 2022, 24,6338

How stable are nanosized AnO_2 compounds against oxidation?

Karlsruhe Institute of Technology

Charge compensation mechanism:
U(V) ➡ U(IV) and Am(IV) ➡ Am(III)

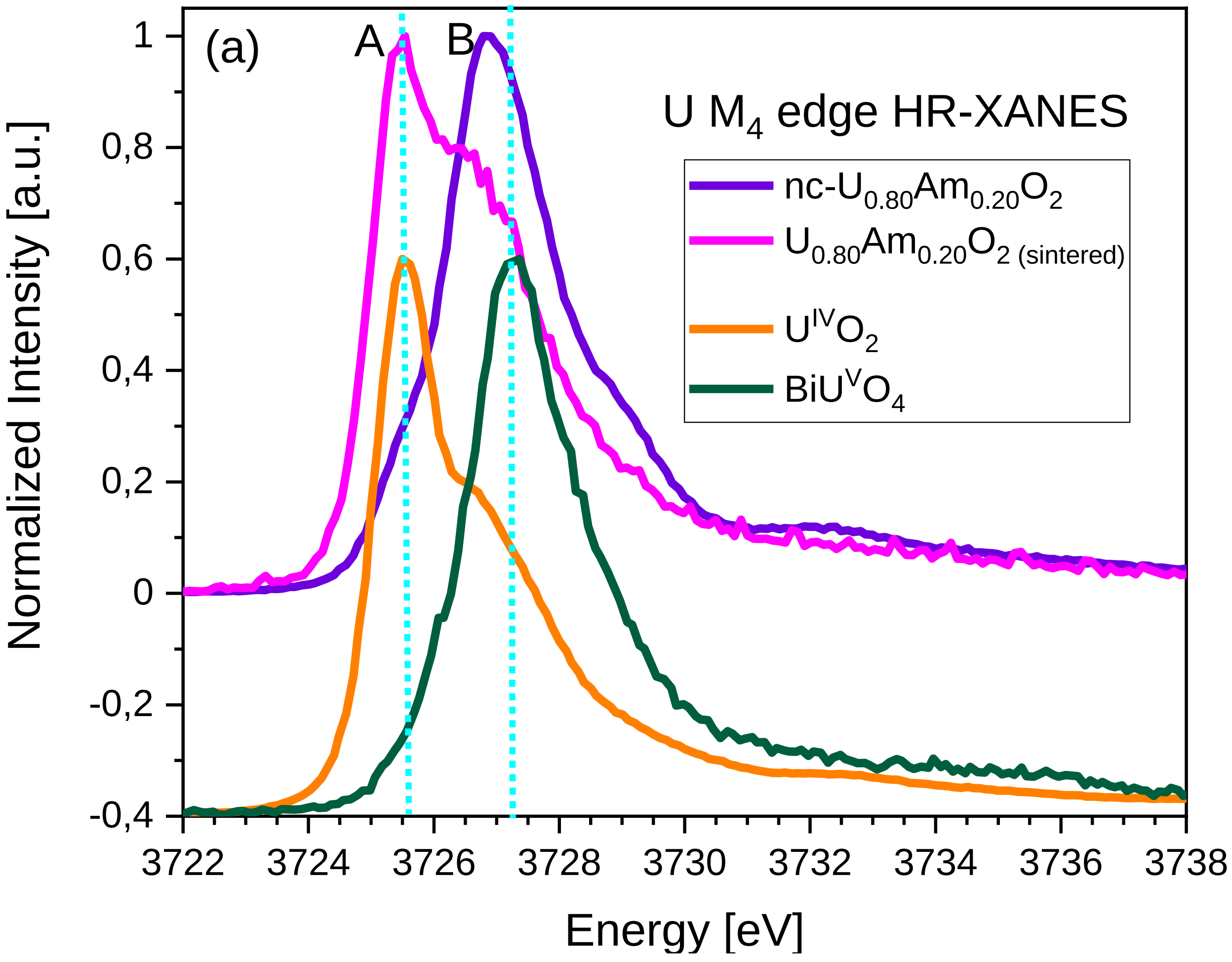

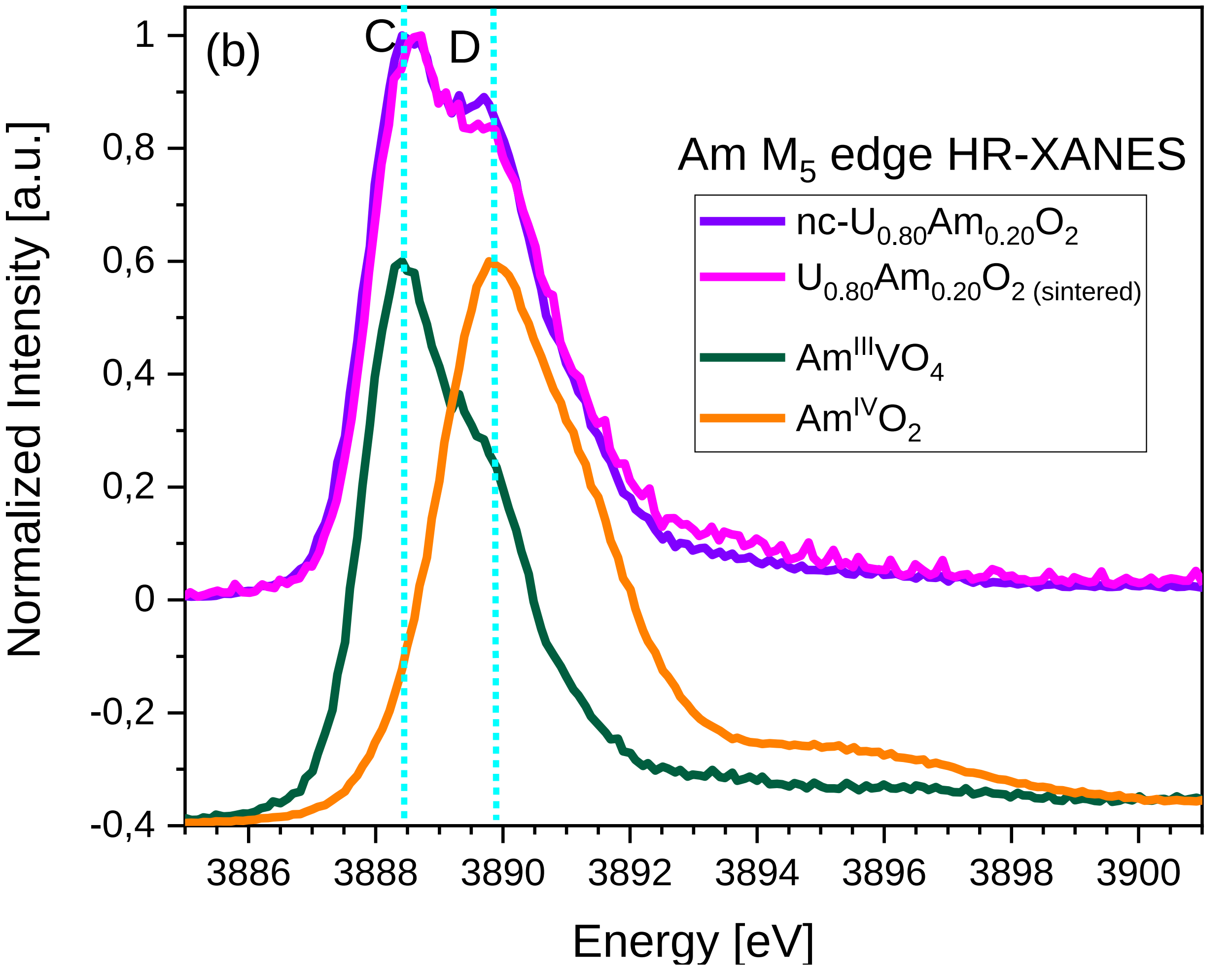

J.F. Vigier, O. Walter, T.Vitova, K. Popa et al. CrystEngComm, 2022, 24,6338

E. Epifano et al.,Communications Chemistry 2 (2019) 59

Literature

Karlsruhe Institute of Technology

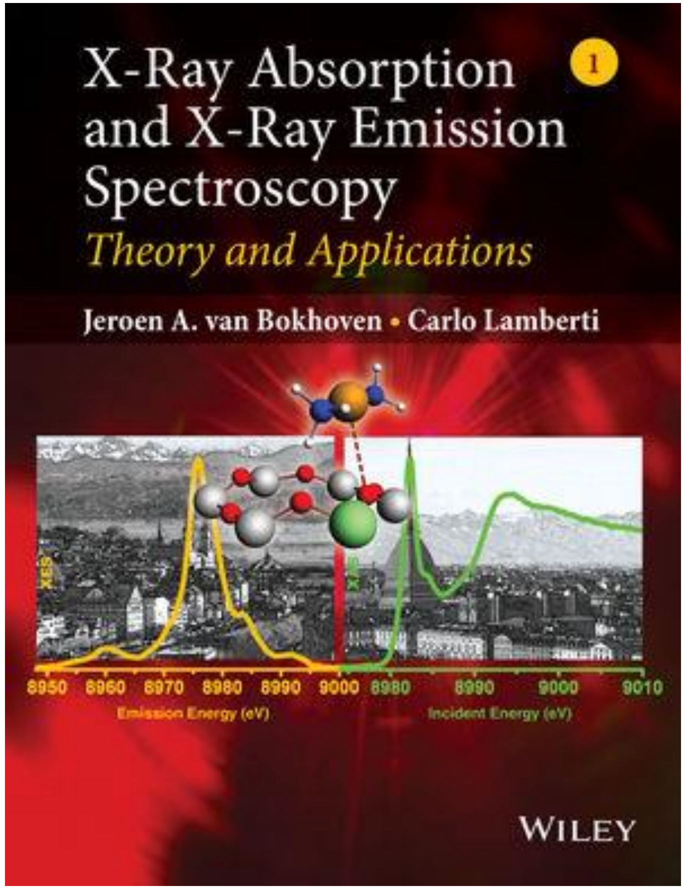

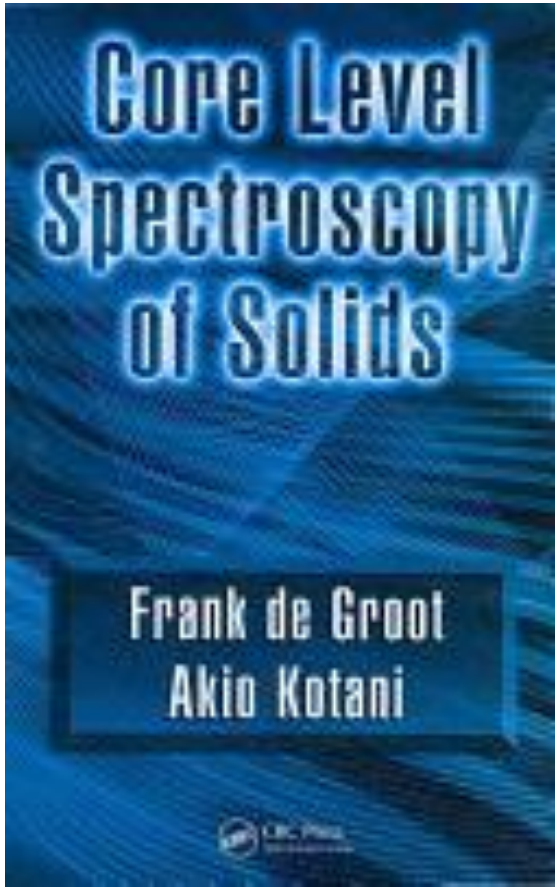

March 2016
http://onlinelibrary.wiley.com/book/10.1002/9781118844243